

Spatiotemporal pattern formation of Beddington-DeAngelis-type predator-prey model

Weiming Wang* and Lei Zhang

Institute of Nonlinear Analysis, College of Mathematics and Information Science,

Wenzhou University, Wenzhou, Zhejiang, 325035 and

Department of Mathematics, North University of China, Taiyuan, Shan'xi 030051, P.R. China

Yakui Xue and Zhen Jin

Department of Mathematics, North University of China, Taiyuan, Shan'xi 030051, P.R. China

(Dated: September 5, 2021)

In this paper, we investigate the emergence of a predator-prey model with Beddington-DeAngelis-type functional response and reaction-diffusion. We derive the conditions for Hopf and Turing bifurcation on the spatial domain. Based on the stability and bifurcation analysis, we give the spatial pattern formation via numerical simulation, i.e., the evolution process of the model near the coexistence equilibrium point. We find that for the model we consider, pure Turing instability gives birth to the spotted pattern, pure Hopf instability gives birth to the spiral wave pattern, and both Hopf and Turing instability give birth to stripe-like pattern. Our results show that reaction-diffusion model is an appropriate tool for investigating fundamental mechanism of complex spatiotemporal dynamics. It will be useful for studying the dynamic complexity of ecosystems.

PACS numbers: 87.23.Cc, 89.75.Kd, 89.75.Fb, 47.54.-r

Keywords: Reaction-diffusion equations; Hopf bifurcation; Turing instability; Spatiotemporal pattern

Contents

1. Introduction	1
2. Stability and bifurcation analysis	3
3. Spatiotemporal pattern formation	7
4. Conclusions and remarks	10
References	11

1. INTRODUCTION

Mathematical models have played an important role throughout the history of ecology. Models in ecology serve a variety of purposes, which range from illustrating an idea to parameterizing a complex real-world situation. They are used to make general predictions, to guide management practices, and to provide a basis for the development of statistical tools and testable hypotheses [10, 40, 51].

A fundamental goal of theoretical ecology is to understand how the interactions of individual organisms with each other and with the environment determine the distribution of populations and the structure of communities [9]. As we know, our ecological environment is a huge and highly complex system. This complexity arises in part from the diversity of biological species, and also from the complexity of every individual organism [29, 30]. The dynamic behavior of predator-prey model has long been and will continue to be one of the dominant themes in both ecology and mathematical ecology due to its universal existence and importance [7, 35].

Before the 1970s, ecological population models typically used ordinary differential equations, seeking equilibria and analyzing stability. The early models provided important insights, such as when species can stably coexist and when predator and prey density oscillate over time [10].

*Electronic address: weimingwang2003@163.com

We live in a spatial world, and spatial patterns are ubiquitous in nature, which modify the temporal dynamics and stability properties of population density at a range of spatial scales, whose effects must be incorporated in temporal ecological models that do not represent space explicitly. And the spatial component of ecological interactions has been identified as an important factor in how ecological communities are shaped [10]. Empirical evidence suggests that the spatial scale and structure of the environment can influence population interactions and the composition of communities [9]. In recent decades, the role of spatial effects in maintaining biodiversity has received a great deal of attention in the literature on conservation [5, 22, 39, 43, 49, 50, 51, 64].

The past investigations have revealed that spatial inhomogeneities like the inhomogeneous distribution of nutrients as well as interactions on spatial scales like migration can have an important impact on the dynamics of ecological populations [50, 51]. In particular it has been shown that spatial inhomogeneities promote the persistence of ecological populations, play an important role in speciation and stabilize population levels [5]. Spatial ecology today is still dominated by theoretical investigations, and empirical studies that explore the role of space are becoming more common due to technological advances that allow the recording of exact spatial locations [10].

In 1952, Alan Turing, one of the key scientists of 20th century, mathematically showed that a system of coupled reaction-diffusion equations could give rise to spatial concentration patterns of a fixed characteristic length from an arbitrary initial configuration due to diffusion-driven instability [61]. The work by Turing belongs to the field of pattern formation, a subfield of mathematical biology. Pattern formation in nonlinear complex systems is one of the central problems of the natural, social, and technological sciences. The occurrence of multiple steady states and transitions from one to another after critical fluctuations, the phenomena of excitability, oscillations, waves and the emergence of macroscopic order from microscopic interactions in various nonlinear nonequilibrium systems in nature and society have been the subject of many theoretical and experimental studies [50]. It has been qualitatively shown that Turing models can indeed imitate biological patterns [37].

The study of biological pattern formation has gained popularity since the 1970s, and Segel and Jackson [56] were the first to apply Turing's ideas to a problem in population dynamics: the dissipative instability in the predator-prey interaction of phytoplankton and herbivorous copepods with higher herbivore motility. At the same time, Gierer and Meinhardt [21] gave a biologically justified formulation of a Turing model and studied its properties by employing numerical simulations. Levin and Segel [41] suggested this scenario of spatial pattern formation was a possible origin of planktonic patchiness.

Spatial patterns and aggregated population distributions are common in nature and in a variety of spatiotemporal models with local ecological interactions [54]. And the understanding of patterns and mechanism of species spatial dispersal is an issue of current interest in conservation biology and ecology [3, 39, 50]. It arises from many ecological applications, and in particular, plays a major role in connection to biological invasion and epidemic spread and so on [3, 5, 10, 19, 39, 43, 47, 48, 50, 51]. The field of research on pattern formation modeled by reaction-diffusion systems, which provides a general theoretical framework for describing pattern formation in systems from many diverse disciplines including biology [9, 34, 36, 39, 45, 50, 53, 54, 58, 63, 64], chemistry [17, 33, 52, 62, 66, 67, 68, 69, 70], physics [12, 31, 38, 60], epidemiology [43, 44] and so on, seems to be a new increasingly interesting area, particularly during the last decade.

In general, a classical predator-prey model can be written as the form [2, 4]:

$$\dot{N} = Nf(N) - Pg(N, P), \quad \dot{P} = h[g(N, P), P]P.$$

where N and P are prey and predator densities, respectively, $f(N)$ the prey growth rate, $g(N, P)$ the functional response, e.g., the prey consumption rate by an average single predator, and $h[g(N, P), P]$ the per capita growth rate of predators (also known as the ‘‘predator numerical response’’), which obviously increases with the prey consumption rate. The most widely accepted assumption for the numerical response is the linear one [2]:

$$h[g(N, P), P] = \varepsilon g(N, P) - \eta$$

where η is a per capita predator death rate and ε the conversion efficiency of food into offspring.

In population dynamics, a functional response $g(N, P)$ of the predator to the prey density refers to the change in the density of prey attached per unit time per predator as the prey density changes [1, 55]. There have been several famous functional response types: Holling types I–III [26, 27]; Hassell-Varley type [25]; Beddington-DeAngelis type by Beddington [6] and DeAngelis *et al* [15] independently; the Crowley-Martin type [13]; and the recent well-known ratio-dependence type by Arditi and Ginzburg [4] later studied by Kuang and Beretta [35]. Of them, the Holling type I-III is labeled ‘‘prey-dependent’’ and other types that consider the interference among predators are labeled ‘‘predator-dependent’’ [4].

In our previous work [64], we studied the spatiotemporal complexity of a ratio-dependent predator-prey model with Michaelis-Menten-type functional response. Compare Michaelis-Menten-type functional response

$$g(N, P) = \frac{\alpha N}{P + \alpha h N}$$

(α, h are positive constants, α capture rate and h handling time) with Beddington-DeAngelis-type functional response

$$g(N, P) = \frac{\beta N}{B + N + wP} \quad (1)$$

(β, B are positive constants, β a maximum consumption rate, B a saturation constant, w a predator interference parameter, a constant. $w < 0$ is the case where predators benefit from cofeeding). Some scholars [2, 46, 59] indicate that where there is a small difference between the denominators, there is a world between them from the biological point.

If predators do not waste time interacting with one another or if their attacks are always successful and instantaneous, i.e., $w = 0$ in (1), then a Holling type II functional response is obtained:

$$g(N) = \frac{\beta N}{B + N}.$$

If $B = 0$ in (1), the Michaelis-Menten-type functional response is obtained.

Furthermore, in [59], by comparing the statistical evidence from nineteen categories of predator-prey systems with three predator-dependent functional responses, Skalski and Gilliam pointed out that the predator-dependent functional responses could provide better descriptions of predator feeding over a range of predator-prey abundance, and in some cases, the Beddington-DeAngelis-type functional response performed even better [46].

Some progress has been seen in the study of predator-prey model with Beddington-DeAngelis-type functional response [2, 8, 14, 16, 18, 20, 28, 29, 32, 42, 46, 65]. However, the research on considering reaction-diffusion to such a model, to our knowledge, seems rare.

In this paper, we report a study of Turing pattern formation in a two-species reaction-diffusion predator-prey model with Beddington-DeAngelis-type functional response. In the next section we give a brief stability and bifurcation analysis of the model. Then, we present and discuss the results of numerical simulations, which is followed by the last section, i.e., conclusions and remarks.

2. STABILITY AND BIFURCATION ANALYSIS

In this paper, we mainly focus on the following predator-prey model with Beddington-DeAngelis-type functional response and reaction-diffusion:

$$\frac{\partial N}{\partial t} = r \left(1 - \frac{N}{K}\right) N - \frac{\beta N}{B + N + wP} P + d_1 \nabla^2 N, \quad \frac{\partial P}{\partial t} = \frac{\varepsilon \beta N}{B + N + wP} P - \eta P + d_2 \nabla^2 P. \quad (2)$$

where t denotes time and N, P stand for prey and predator density, respectively. All parameters are positive constants, r standing for maximum per capita growth rate of the prey, β capture rate, η predator death rate, w a predator interference parameter and K carrying capacity, which is the nonzero equilibrium population size. The diffusion coefficients are denoted by d_1 and d_2 , respectively. $\nabla^2 = \frac{\partial}{\partial x^2} + \frac{\partial}{\partial y^2}$ is the usual Laplacian operator in two-dimensional space.

The first step in analyzing the model is to determine the equilibria (stationary states) of the non-spatial model obtained by setting space derivatives equal to zero, i.e.,

$$r \left(1 - \frac{N}{K}\right) N - \frac{\beta N}{B + N + wP} P = 0, \quad \frac{\varepsilon \beta N}{B + N + wP} P - \eta P = 0. \quad (3)$$

In fact, physically, an equilibrium represents a situation without “life”. It may mean no motion of a pendulum, no reaction in a reactor, no nerve activity, no flutter of an airfoil, no laser operation, or no circadian rhythms of biological clocks [57]. And at each equilibrium point, the movement of the population dynamics vanishes.

Eqs.(3) has at most three equilibria, which correspond to spatially homogeneous equilibria of the full model, Eq.(2), in the positive quadrant:

(i) $(0, 0)$ (total extinct) is a saddle point.

- (ii) $(K, 0)$ (extinct of the predator, or prey-only) is a stable node if $\varepsilon\beta < \eta$ or if $\varepsilon\beta > \eta$ and $K < \frac{\eta B}{\varepsilon\beta - \eta}$; a saddle if $\varepsilon\beta < \eta$ and $K > \frac{\eta B}{\varepsilon\beta - \eta}$; a saddle-node if $\varepsilon\beta < \eta$ and $K = \frac{\eta B}{\varepsilon\beta - \eta}$.
- (iii) a nontrivial stationary state (N^*, P^*) (coexistence of prey and predator), where

$$N^* = \frac{1}{2rw\varepsilon} \left(K(rw\varepsilon - \varepsilon\beta + \eta) + \sqrt{K^2(rw\varepsilon - \varepsilon\beta + \eta)^2 + 4rKw\varepsilon\eta B} \right),$$

$$P^* = \frac{(\beta\varepsilon - \eta)}{w\eta} N^* - \frac{B}{w}.$$

To perform a linear stability analysis, we linearize the dynamic system 2 around the equilibrium point (N^*, P^*) for small space- and time-dependent fluctuations and expand them in Fourier space

$$N(\vec{x}, t) \sim N^* e^{\lambda t} e^{i\vec{k}\cdot\vec{x}}, \quad P(\vec{x}, t) \sim P^* e^{\lambda t} e^{i\vec{k}\cdot\vec{x}},$$

and obtain the characteristic equation

$$|A - k^2 D - \lambda I| = 0, \quad (4)$$

where $D = \text{diag}(d_1, d_2)$ and the Jacobian matrix A is given by

$$A = \begin{pmatrix} \partial_n f & \partial_p f \\ \partial_n g & \partial_p g \end{pmatrix}_{(N^*, P^*)} = \begin{pmatrix} f_n & f_p \\ g_n & g_p \end{pmatrix}.$$

Now Eq.(4) can be solved, yielding the so called characteristic polynomial of the original problem (2):

$$\lambda^2 - \text{tr}_k \lambda + \Delta_k = 0, \quad (5)$$

where

$$\text{tr}_k = f_n + g_p - k^2(d_1 + d_2) = \text{tr}_0 - k^2(d_1 + d_2),$$

$$\Delta_k = f_n g_p - f_p g_n - k^2(f_n d_2 + g_p d_1) + k^4 d_1 d_2 = \Delta_0 - k^2(f_n d_2 + g_p d_1) + k^4 d_1 d_2.$$

The roots of Eq.(5) yield the dispersion relation

$$\lambda(k) = \frac{1}{2} \left(\text{tr}_k \pm \sqrt{\text{tr}_k^2 - 4\Delta_k} \right). \quad (6)$$

We know that one type of instability (or bifurcation) will break one type of symmetry of a system, i.e., in the bifurcation point, two equilibrium states intersect and exchange their stability. Biologically speaking, this bifurcation corresponds to a smooth transition between equilibrium states. The Hopf bifurcation is space-independent and it breaks the temporal symmetry of a system and gives rise to oscillations that are uniform in space and periodic in time. The Turing bifurcation breaks spatial symmetry, leading to the formation of patterns that are stationary in time and oscillatory in space.

The Hopf instability or bifurcation is an important instability in reaction-diffusion systems for which the conditions result in a stable limit cycle (oscillations). In terms of the linearized problem (Eq.4) the onset of Hopf instability corresponds to the case, when a pair of imaginary eigenvalues cross the real axis from the negative to the positive side. The Hopf bifurcation of an equilibrium state is reflected by a transition between stationary and periodic behavior. If the system is in a stable equilibrium before the bifurcation, the stability is lost at the bifurcation point. As a result the system abundance of species start to oscillate periodically. And this situation occurs only when the diffusion vanishes. Mathematically speaking, the Hopf bifurcation occurs when $\text{Im}(\lambda(k)) \neq 0$, $\text{Re}(\lambda(k)) = 0$ at $k = 0$. Then we can get the critical value of the transition, Hopf bifurcation parameter— K , equals

$$K_H = \frac{B(w\varepsilon\eta - \beta\varepsilon - \eta)^2}{(w\varepsilon - 1)(\eta^2 - \beta^2\varepsilon^2 + rw\varepsilon^2\beta + \varepsilon^2\beta w\eta - w\varepsilon\eta^2)} \quad (7)$$

At the Hopf bifurcation threshold, the temporal symmetry of the system is broken and gives rise to uniform oscillations in space and periodic oscillations in time with the frequency

$$\omega_H = \text{Im}(\lambda(k)) = \sqrt{\Delta_0},$$

where

$$\Delta_0 = -\frac{(K(\eta-\beta\varepsilon)(K(rw\varepsilon-\beta\varepsilon+\eta)^2+\eta\delta-\beta\delta\varepsilon+4rw\varepsilon\eta B+r\delta\varepsilon w)+2r\delta\eta B\varepsilon w)_\eta}{\beta K\varepsilon^2 w(rKw\varepsilon-\beta K\varepsilon+K\eta+\delta)},$$

and

$$\delta = \left(r^2 K^2 w^2 \varepsilon^2 - 2 r K^2 w \varepsilon^2 \beta + 2 r K^2 w \varepsilon \eta + \beta^2 K^2 \varepsilon^2 - 2 \beta K^2 \varepsilon \eta + K^2 \eta^2 + 4 r w \varepsilon K \eta B \right)^{1/2}.$$

The corresponding wavelength is

$$\lambda_H = \frac{2\pi}{\omega_H} = \frac{2\pi}{\sqrt{\Delta_0}}.$$

The Turing instability is not dependent upon the geometry of the system but only upon the reaction rates and diffusion. And it cannot be expected when the diffusion term is absent and it can occur only when the activator (e.g., N) diffuses more slowly than the inhibitor (e.g., P). Linear analysis above shows that the necessary conditions for yielding Turing patterns are given by

$$f_n + g_p < 0, \quad f_n g_p - f_p g_n > 0, \quad d_2 g_p + d_1 f_n > 0, \quad (d_2 f_n + d_1 g_p)^2 > 4 d_1 d_2 (f_n g_p - f_p g_n).$$

Mathematically speaking, as $d_1 \ll d_2$, the Turing bifurcation occurs when

$$\text{Im}(\lambda(k)) = 0, \quad \text{Re}(\lambda(k)) = 0 \text{ at } k = k_T \neq 0,$$

and the wavenumber k_T satisfies $k_T^2 = \sqrt{\frac{\Delta_0}{d_1 d_2}}$. At the Turing bifurcation threshold, the spatial symmetry of the system is broken and the patterns are stationary in time and oscillatory in space with the corresponding wavelength

$$\lambda_T = \frac{2\pi}{k_T}. \quad (8)$$

And the critical value of Turing bifurcation parameter K takes the following form:

$$K_T = \frac{F_1 A + F_2}{G_1 A + G_2}, \quad (9)$$

where

$$\begin{aligned} A &= (-\eta d_1 (\varepsilon \beta - \eta) (-\varepsilon d_2 \beta - \eta d_2 + \varepsilon w \eta d_1))^2 (-\varepsilon \eta d_1 r w - \varepsilon \eta d_1 \beta + \varepsilon r^2 d_2 w - \varepsilon r d_2 \beta + d_1 \eta^2 - r d_2 \eta)^{1/2}, \\ F_1 &= -(\eta^2 (d_1 \varepsilon w - d_2)^2 + \varepsilon d_2 \beta (\varepsilon d_2 \beta + 2 \eta d_2 + 6 \varepsilon w \eta d_1))^2 ((-2 \varepsilon^2 \beta w d_2 (2 w \varepsilon \eta^2 d_1 d_2 - 4 w \varepsilon^2 \eta d_1 d_2 \beta - \eta^2 d_1^2 \varepsilon^2 w^2 \\ &\quad + \beta^2 d_2^2 \varepsilon^2 - d_2^2 \eta^2) r) + 2 \varepsilon d_2 \beta (\varepsilon \beta - \eta) (\varepsilon^2 (d_2 \beta + w \eta d_1)^2 + \eta d_2 (\eta d_2 - 2 \varepsilon w \eta d_1 + 2 \varepsilon d_2 \beta))) r B, \\ F_2 &= -(\eta^2 (d_1 \varepsilon w - d_2)^2 + \varepsilon d_2 \beta (\varepsilon d_2 \beta + 2 \eta d_2 + 6 \varepsilon w \eta d_1))^2 (\eta \beta \varepsilon^2 w d_2 (\varepsilon d_2 \beta + \eta d_2 - \varepsilon w \eta d_1) (\varepsilon^3 d_1 w (3 d_2 \beta + w \eta d_1)^2 \\ &\quad + d_2^3 (\eta + \varepsilon \beta)^2 - \varepsilon d_1 \eta^2 w d_2 (d_1 \varepsilon w + d_2)) r^2 - \eta (\varepsilon \beta - \eta) (\varepsilon d_2 \beta + \eta d_2 - \varepsilon w \eta d_1) (\varepsilon^4 \eta^3 w^4 d_1^4 + \varepsilon^3 \eta^2 w^3 d_2 (-4 \eta \\ &\quad + 9 \varepsilon \beta) d_1^3 + 3 \varepsilon^2 \eta w^2 d_2^2 (-5 \eta \varepsilon \beta + 2 \eta^2 + 9 \varepsilon^2 \beta^2) d_1^2 + \varepsilon w d_2^3 (11 \varepsilon \beta - 4 \eta) (\eta + \varepsilon \beta)^2 d_1 + d_2^4 (\eta + \varepsilon \beta)^3) r \\ &\quad + 2 \eta \beta d_1 \varepsilon d_2 (\varepsilon \beta - \eta)^2 (\varepsilon d_2 \beta + \eta d_2 - \varepsilon w \eta d_1) (\varepsilon^2 (d_2 \beta + w \eta d_1)^2 + \eta d_2 (\eta d_2 - 2 \varepsilon w \eta d_1 + 2 \varepsilon d_2 \beta))) r B, \\ G_1 &= G_{11} G_{12}, \\ G_{11} &= 4 \varepsilon d_2 \beta (-(\varepsilon^2 \beta d_2 (d_2 \beta - 4 w \eta d_1) - \eta^2 (d_1 \varepsilon w - d_2)^2) w \varepsilon r + (\varepsilon \beta - \eta) (\varepsilon^2 (d_2 \beta + w \eta d_1)^2 + \eta d_2 (\eta d_2 - 2 \varepsilon w \eta d_1 \\ &\quad + 2 \varepsilon d_2 \beta))), \\ G_{12} &= (\varepsilon^3 d_1 w (3 d_2 \beta + w \eta d_1)^2 + d_2^3 (\eta + \varepsilon \beta)^2 - \varepsilon d_1 \eta^2 w d_2 (d_1 \varepsilon w + d_2)) d_2 w \beta \varepsilon^2 r^2 - (\varepsilon \beta - \eta) (\varepsilon^3 d_2^3 (d_2 + 11 d_1 \varepsilon w) \beta^3 \\ &\quad + 3 d_2^2 \eta \varepsilon^2 (3 d_1 \varepsilon w + d_2)^2 \beta^2 + 3 \varepsilon \eta^2 d_2 (3 d_1 \varepsilon w + d_2) (d_1 \varepsilon w - d_2)^2 \beta + \eta^3 (d_1 \varepsilon w - d_2)^4) r + 2 \varepsilon \beta d_1 d_2 (\varepsilon \beta - \eta)^2 \\ &\quad (\varepsilon^2 (d_2 \beta + w \eta d_1)^2 + \eta d_2 (\eta d_2 - 2 \varepsilon w \eta d_1 + 2 \varepsilon d_2 \beta)), \\ G_2 &= G_{21} G_{22}, \\ G_{21} &= \varepsilon d_2 \beta + \eta d_2 - \varepsilon w \eta d_1, \\ G_{22} &= g_0 + g_1 r + g_2 r^2 + g_3 r^3 + g_4 r^4, \\ g_0 &= 8 \varepsilon^2 \beta^2 \eta d_1^2 d_2^2 (\varepsilon \beta - \eta)^4 (\varepsilon^2 (d_2 \beta + w \eta d_1)^2 - 2 \varepsilon d_1 \eta^2 w d_2 + d_2^2 \eta^2 + 2 \beta \varepsilon \eta d_2^2)^2, \\ g_1 &= 4 \varepsilon \beta d_1 d_2 (\varepsilon \beta - \eta)^3 (\varepsilon^2 (d_2 \beta + w \eta d_1)^2 - 2 \varepsilon d_1 \eta^2 w d_2 + d_2^2 \eta^2 + 2 \beta \varepsilon \eta d_2^2) (- (d_1 \varepsilon w - d_2)^4 \eta^4 - 2 \varepsilon \beta d_2 (3 d_1 \varepsilon w + d_2) \\ &\quad (d_1 \varepsilon w - d_2)^2 \eta^3 - 16 \varepsilon^3 \beta^2 d_1 w d_2^2 (d_1 \varepsilon w + d_2) \eta^2 - 2 \varepsilon^3 d_2^3 \beta^3 (-d_2 + 5 d_1 \varepsilon w) \eta + d_2^4 \varepsilon^4 \beta^4), \end{aligned}$$

$$\begin{aligned}
g_2 &= (\varepsilon\beta - \eta)^2((d_1\varepsilon w - d_2)^8\eta^7 + 6\varepsilon\beta d_2(3d_1\varepsilon w + d_2)(d_1\varepsilon w - d_2)^6\eta^6 + \beta^2 d_2^2 \varepsilon^2(151\varepsilon^2 w^2 d_1^2 + 106\varepsilon d_1 w d_2 + 15d_2^2) \\
&\quad (d_1\varepsilon w - d_2)^4\eta^5 + 4\varepsilon^3 d_2^3 \beta^3(156\varepsilon^3 d_1^3 w^3 + 133\varepsilon^2 w^2 d_1^2 d_2 + 58 w d_1 \varepsilon d_2^2 + 5d_2^3)(d_1\varepsilon w - d_2)^2\eta^4 + d_2^4 \varepsilon^4 \beta^4(3d_1\varepsilon w \\
&\quad + d_2)(389\varepsilon^3 d_1^3 w^3 + 117\varepsilon^2 w^2 d_1^2 d_2 + 183 w d_1 \varepsilon d_2^2 + 15d_2^3)\eta^3 + 2\varepsilon^5 \beta^5 d_2^5(357\varepsilon^3 d_1^3 w^3 + 297\varepsilon^2 w^2 d_1^2 d_2 \\
&\quad + 47 w d_1 \varepsilon d_2^2 + 3d_2^3)\eta^2 + \varepsilon^6 \beta^6 d_2^6(153\varepsilon^2 w^2 d_1^2 + d_2^2 - 10\varepsilon d_1 w d_2)\eta - 12\varepsilon^8 \beta^7 w d_1 d_2^7), \\
g_3 &= -2\varepsilon^2 \beta w d_2(\varepsilon\beta - \eta)((d_1\varepsilon w + d_2)(d_1\varepsilon w - d_2)^6\eta^6 + \varepsilon\beta d_2(13\varepsilon^2 w^2 d_1^2 + 6\varepsilon d_1 w d_2 + 5d_2^2)(d_1\varepsilon w - d_2)^4\eta^5 \\
&\quad + 2\beta^2 d_2^2 \varepsilon^2(38\varepsilon^3 d_1^3 w^3 + \varepsilon^2 w^2 d_1^2 d_2 + 20 w d_1 \varepsilon d_2^2 + 5d_2^3)(d_1\varepsilon w - d_2)^2\eta^4 + 2\varepsilon^3 \beta^3 d_2^3(5d_2^4 + 117\varepsilon^4 w^4 d_1^4 \\
&\quad + 44\varepsilon d_1 w d_2^3 + 14d_2^2 d_1^2 w^2 \varepsilon^2 - 52d_2 d_1^3 w^3 \varepsilon^3)\eta^3 + d_2^4 \varepsilon^4 \beta^4(227\varepsilon^2 w^2 d_1^2 d_2 + 329\varepsilon^3 d_1^3 w^3 + 79 w d_1 \varepsilon d_2^2 \\
&\quad + 5d_2^3)\eta^2 + \varepsilon^5 \beta^5 d_2^5(14\varepsilon d_1 w d_2 + d_2^2 + 121\varepsilon^2 w^2 d_1^2)\eta - 6\varepsilon^7 d_1 w d_2^6 \beta^6), \\
g_4 &= \varepsilon^4 \beta^2 w^2 d_2^2((\varepsilon^2 w^2 d_1^2 + 6\varepsilon d_1 w d_2 + d_2^2)(w d_1 \varepsilon - d_2)^4\eta^5 + 4\varepsilon\beta d_2(2\varepsilon^3 d_1^3 w^3 + 13\varepsilon^2 w^2 d_1^2 d_2 + d_2^3)(w d_1 \varepsilon - d_2)^2\eta^4 \\
&\quad + 2\beta^2 d_2^2 \varepsilon^2(3d_2^4 + 52d_2 d_1^3 w^3 \varepsilon^3 - 6d_2^2 d_1^2 w^2 \varepsilon^2 + 4\varepsilon d_1 w d_2^3 + 11\varepsilon^4 w^4 d_1^4)\eta^3 + 4\varepsilon^3 \beta^3 d_2^3(-9\varepsilon^2 w^2 d_1^2 d_2 + d_2^3 \\
&\quad + 13\varepsilon^3 d_1^3 w^3 + 11 w d_1 \varepsilon d_2^2)\eta^2 + d_2^4 \varepsilon^4 \beta^4(113\varepsilon^2 w^2 d_1^2 + d_2^2 + 22\varepsilon d_1 w d_2)\eta - 4d_2^5 \varepsilon^6 w d_1 \beta^5),
\end{aligned}$$

In the following, linear stability analysis yields the bifurcation diagram with $r = 0.5$, $\varepsilon = 1$, $\beta = 0.6$, $B = 0.4$, $\eta = 0.25$, $w = 0.4$, $d_2 = 1$ shown in Fig. 1(A).

The Hopf bifurcation line and the Turing bifurcation curve separate the parametric space into four distinct domains. In domain I, located below all two bifurcation lines, the steady state is the only stable solution of the system. Domain II is the region of pure Turing instability, while domain III is the region of pure Hopf instability. In domain IV, which is located above all two bifurcation lines, both Hopf and Turing instability occur.

To see the relation between the real and the imaginary parts of the eigenvalue $\lambda(k)$, we plot in Fig. 1(B)–(F) the real and the imaginary parts of the eigenvalue at different K with $r = 0.5$, $\varepsilon = 1$, $\beta = 0.6$, $B = 0.4$, $\eta = 0.25$, $w = 0.4$, $d_1 = 0.01$ and $d_2 = 1$ for the system 2.

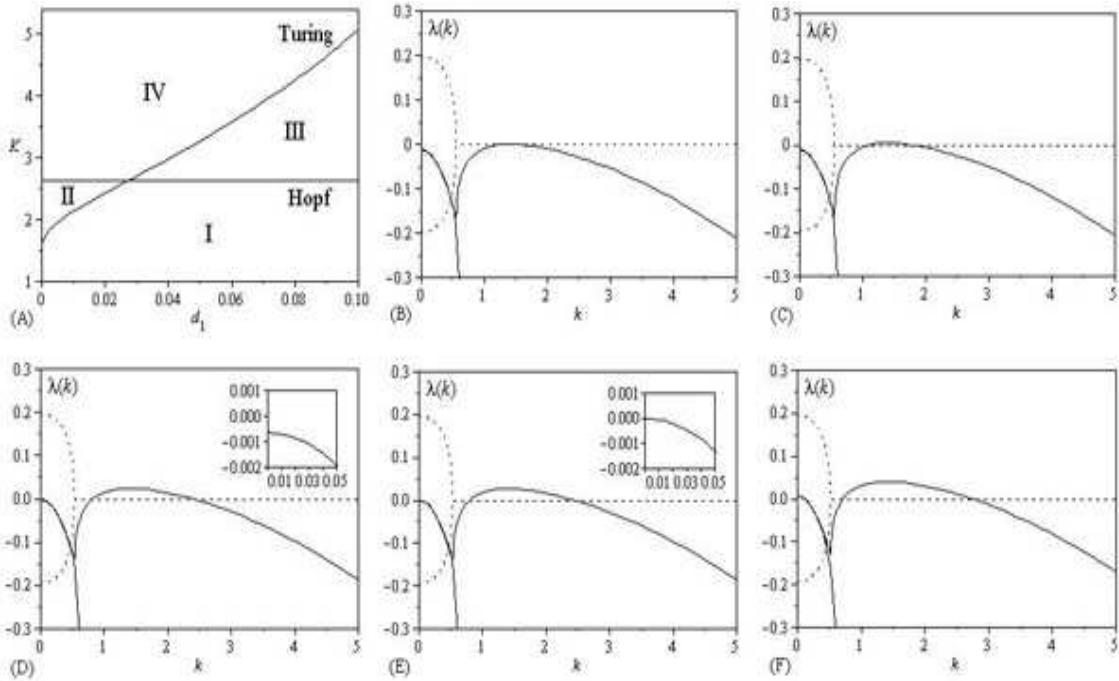


FIG. 1: (A) $K - d_1$ Bifurcation diagram for the model 2 with $r = 0.5$, $\varepsilon = 1$, $\beta = 0.6$, $B = 0.4$, $\eta = 0.25$, $w = 0.4$ and $d_2 = 1$. Hopf and Turing bifurcation lines separate the parameter space into four domains. And the Hopf-Turing bifurcation point is $(d_1, K) = (0.02742, 2.63158)$. In (B)–(F), $\text{Re}(\lambda(k))$ and $\text{Im}(\lambda(k))$ are shown by solid curves and dotted curves, respectively. The other parameters are: $d_1 = 0.01$, the bifurcation parameter K : (B) 2.131712170, the critical value of K_T ; (C) 2.2; (D) 2.6; (E) 2.631578947 the critical value of K_H ; (F) 3.0.

From the definition of Hopf and Turing bifurcation, we know that the relation between the real, the imaginary parts of the eigenvalue $\lambda(k)$ determine the bifurcation type. The relation between $\text{Re}(\lambda(k))$, $\text{Im}(\lambda(k))$ and k are shown in

figure 1(B)–(F). Figure 1(B) illustrate the case of parameter locate in domain I in figure 1(A), $K = 2.131712170$, the critical value of Turing bifurcation, in this case, $\text{Re}(\lambda(k)) > 0$ at $k = 0$ while $\text{Im}(\lambda(k)) \neq 0$. In figure 1(C)(D), $K = 2.2$ and $K = 2.6$, the parameter locate in domain II, the pure Turing instability occurs, one can see that at $k = 0$, $\text{Re}(\lambda(k)) = 0$, $\text{Im}(\lambda(k)) \neq 0$. Figure 1(E), $K = 2.631578947$, the critical value of Hopf bifurcation, in this case, $\text{Re}(\lambda(k)) = 0$ at $k = 0$ while $\text{Im}(\lambda(k)) \neq 0$. When $K = 3.0$, parameter locate in domain IV, figure 1(F) indicate that at $k = 0$, $\text{Re}(\lambda(k)) > 0$, $\text{Im}(\lambda(k)) \neq 0$.

3. SPATIOTEMPORAL PATTERN FORMATION

In this section, we perform extensive numerical simulations of the spatially extended model (2) in two-dimensional spaces, and the qualitative results are shown here. All our numerical simulations employ the periodic Neumann (zero-flux) boundary conditions with a system size of 200×200 space units and $r = 0.5$, $\varepsilon = 1$, $\beta = 0.6$, $B = 0.4$, $\eta = 0.25$, $w = 0.4$ $d_1 = 0.01$ and $d_2 = 1$. The Eq.2 are solved numerically in two-dimensional space using a finite difference approximation for the spatial derivatives and an explicit Euler method for the time integration with a time stepsize of $\Delta t = 0.01$ and space stepsize (lattice constant) $\Delta h = 0.25$ (see, for details, [19]). The scale of the space and time are average to the Euler method. The initial density distribution corresponds to random perturbations around the stationary state (N^*, P^*) in model (2) with a variance significantly lower than the amplitude of the final patterns, which seems to be more general from the biological point of view. When the system reached a stable state (stationary or oscillatory), we took a snapshot with yellow levels linearly proportional to the free species density and red corresponding to high while blue corresponding to low.

In the numerical simulations, different types of dynamics are observed and we have found that the distributions of predator and prey are always of the same type. Consequently, we can restrict our analysis of pattern formation to one distribution. In this section, we show the distribution of prey, for instance.

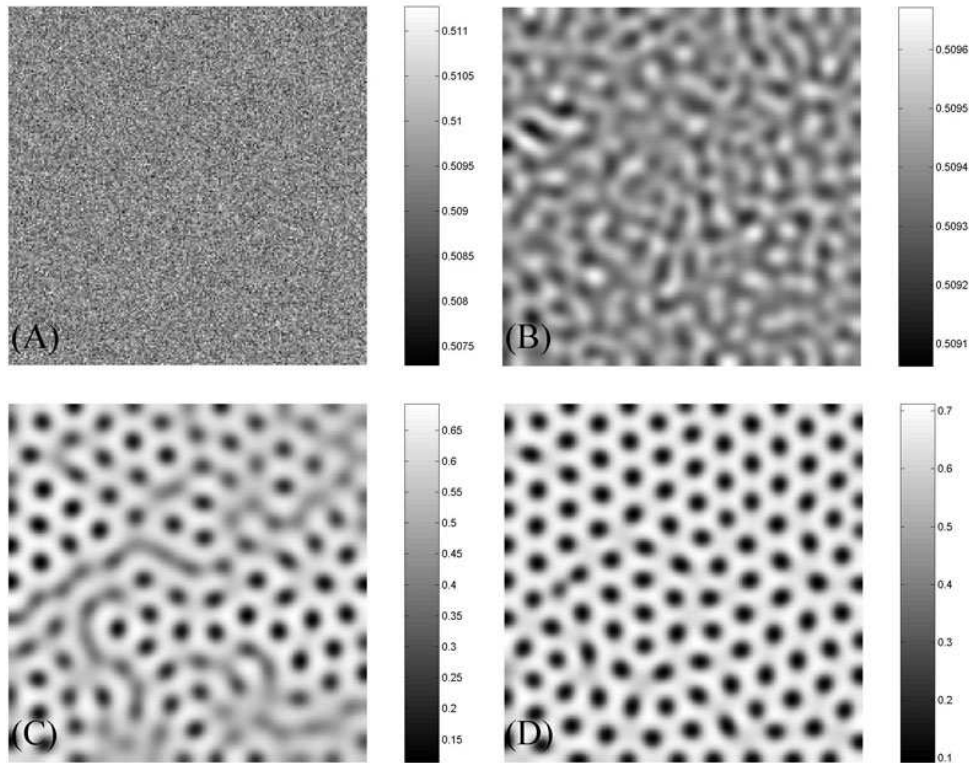


FIG. 2: Dynamics of the time evolution of the prey of model 2 with $d_1 = 0.01$, $K_T < K = 2.2 < K_H$. (A) 0 iteration, (B) 10000 iterations, (C) 200000 iterations, (D) 300000 iterations.

Fig. 2 shows the evolution of the spatial pattern of prey at 0, 10000, 200000 and 300000 iterations, with random small perturbation of the stationary solution $(N^*, P^*) = (0.5094, 0.7829)$ of the spatially homogeneous systems when

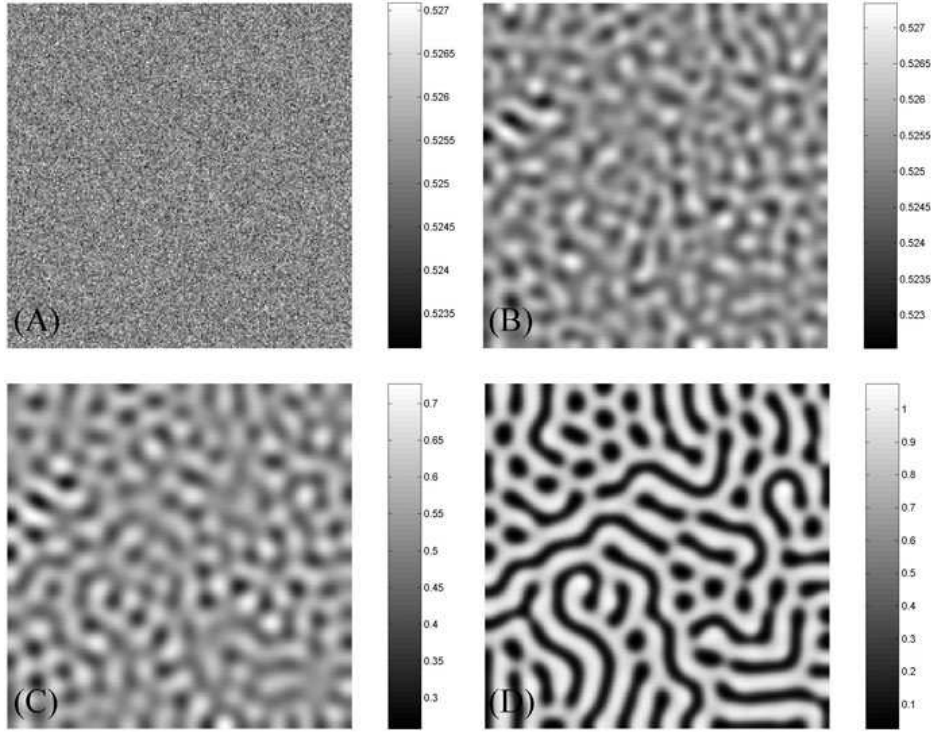


FIG. 3: Dynamics of the time evolution of the prey of model 2 with $d_1 = 0.01$, $K_T < K = 2.6 < K_H$. (A) 0 iteration, (B) 10000 iterations, (C) 30000 iterations, (D) 100000 iterations.

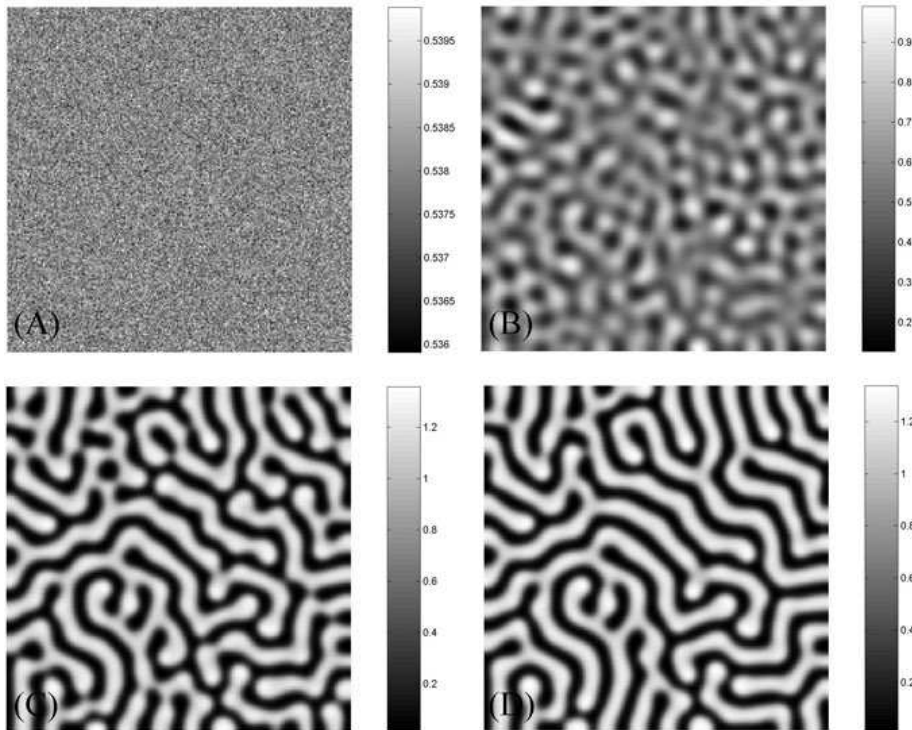


FIG. 4: Dynamics of the time evolution of the prey of model 2 with $d_1 = 0.01$, $K_T < K_H < K = 3.0$. (A) 0 iteration, (B) 20000 iterations, (C) 50000 iterations, (D) 100000 iterations.

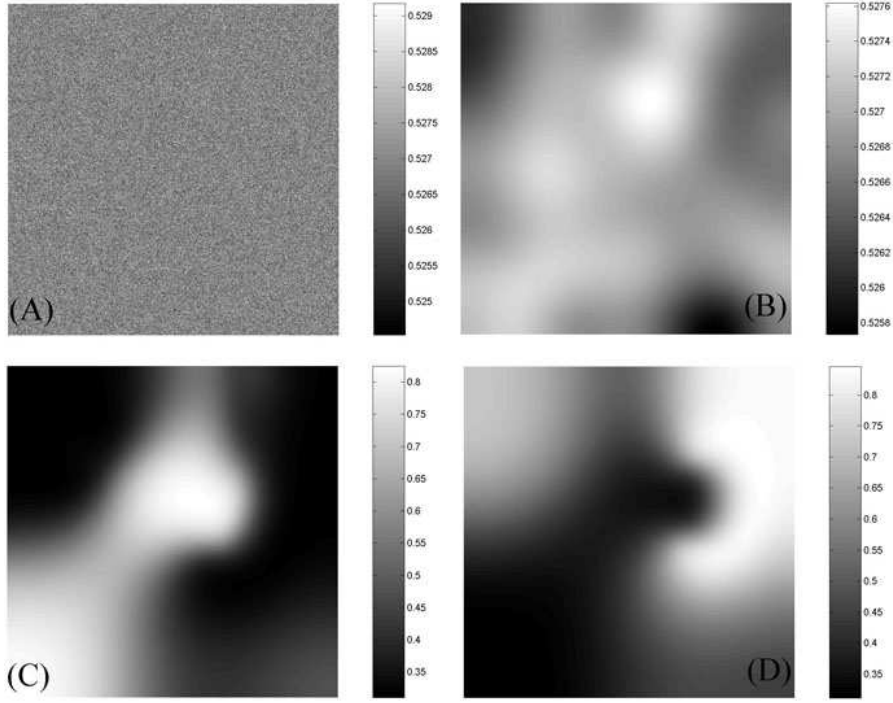


FIG. 5: Dynamics of the time evolution of the prey of model 2 with $d_1 = 0.04$, $K_T < K_H < K = 2.65$. (A) 0 iteration, (B) 30000 iterations, (C) 70000 iterations, (D) 100000 iterations.

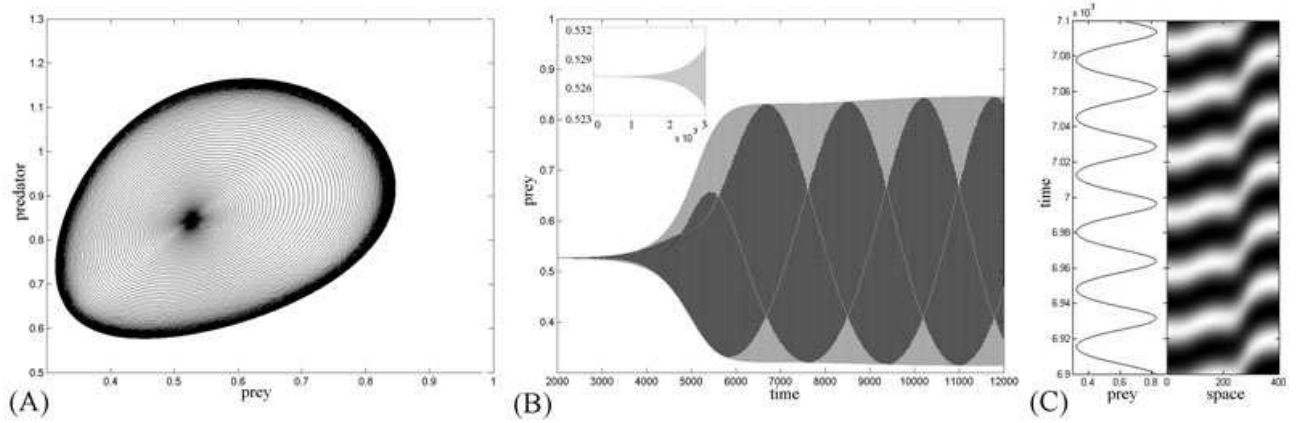


FIG. 6: Dynamical behaviors of model 2. (A) Phase portrait; (B) Time-series plot; (C) Space-time plots corresponding to Fig. 5(C). The parameters are the same as those in Fig 5.

$K = 2.2$, located in domain II, slightly more than the Turing bifurcation threshold $K_T = 2.1317$ and less than the Hopf bifurcation threshold $K_H = 2.6316$. In this case, one can see that for model 2, the random initial distribution (c.f., Fig. 2(A)) leads to the formation of a regular macroscopic spotted pattern which prevails over the whole domain at last, and the dynamics of the system does not undergo any further changes (c.f., Fig. 2(D)).

Fig. 3 shows the evolution of the spatial pattern of prey at 0, 10000, 30000 and 100000 iterations when $K = 2.6$ which is more than K_T and slightly less than K_H . Although the dynamics of the system starts from the stationary solution $(N^*, P^*) = (0.5252, 0.8382)$, there is an essential difference in the case above. From the snapshots, one can see that the steady state of spotted pattern and the stripe-like pattern coexist (c.f., Fig. 3(D)).

In Fig. 4, $K_H < K = 3.0$, i.e., parameters in domain IV, both Hopf and Turing instability occur. In this case, $(N^*, P^*) = (0.5380, 0.8831)$. One can see that the evolution of the spatial pattern of prey at 0, 20000, 50000 and 100000 iterations. After the spatial chaos patterns (c.f., Fig. 4(B)), a regular stationary stripe-like spatial state

emerges (c.f., Fig. 4(D)).

When $K = 2.65$, $d_1 = 0.04$, i.e., parameters in domain III (c.f., Fig. 1(A)), pure Hopf instability occurs. As an example, the formation of a regular macroscopic two-dimensional spatial pattern, the spiral pattern, is shown in Fig. 5 with a system size of 400×400 space units. One can see that for model 2, the random initial distribution around the steady state $(N^*, P^*) = (0.5270, 0.8443)$, a unstable focus of model 2, leads to the formation of the spiral pattern in the domain (c.f., Fig. 5(D)). In other words, in this situation, spatially uniform steady-state predator-prey coexistence is no longer. Small random fluctuations will be strongly amplified by diffusion, leading to nonuniform population distributions. From the analysis in section II, we find with these parameters in domain III, the pattern formation, i.e., the spiral pattern, arises from pure Hopf instability. In order to make it clearer, in Fig. 6, we show phase portrait (Fig. 6(A)), time series plot (Fig. 6(B)) and space-time plots (Fig. 6(C)), a one-dimensional example corresponding to Fig. 5(C). And the method of space-time plots is that let y be a constant (here, $y = 200$, the center line of each snapshots), from each pattern snapshots, choose the line $y = 200$, and pile these lines in-time-order. The space-time plots show the evolution process of the prey N throughout time t and space x . Fig. 6(A) exhibits the “local” phase plane of the system obtained in a fixed point $(0.5270, 0.8443)$ inside the region invaded by the irregular spatiotemporal oscillations, and the trajectory fills nearly the whole domain inside the limit cycle. Fig. 6(B) illustrates the evolution process of prey density with time, periodic oscillations in time finally. From Fig. 6(C), one can clearly see that a spiral wave emerges, and the system gives rise to uniform oscillations in space and periodic oscillations in time.

Comparing Fig. 2, Fig. 3 with Fig. 4, Fig. 5, we can see that the bifurcation parameter K determines the type of the pattern formation even with the same parameters, e.g., $r, \varepsilon, \beta, B, \eta, w, d_2$. In domain II of Fig. 1(A), the closer K is to K_T , the more distinct the spotted spatial pattern becomes (c.f., Fig. 2(D)). When K is much closer to K_H , the spotted and stripe-like patterns coexist (c.f., Fig. 3(D)). When K is bigger than K_H and far away from the Turing bifurcation value K_T , the distinct stripe-like pattern emerges. When K is bigger than K_H and smaller than K_T , the spiral wave pattern occurs (c.f., Fig. 5(C,D)). So we may draw a conclusion that for model 2 pure Turing instability gives birth to the spotted pattern, pure Hopf bifurcation gives birth to the spiral wave pattern, and both of them give birth to the stripe-like pattern.

4. CONCLUSIONS AND REMARKS

In this paper, we have presented a theoretical analysis of evolutionary processes that involves organisms distribution and their interaction of spatially distributed population with local diffusion. And the numerical simulations were consistent with the predictions drawn from the bifurcation analysis, i.e., Hopf bifurcation and Turing instability. In the domain II of Fig. 1(A), the stationary state of periodic spotted pattern exists when the parameters are near the Turing bifurcation line, while near the Hopf bifurcation line, both the spotted pattern and the stripe-like pattern coexist. When the parameters are located in domain III, pure Hopf instability occurs, and the spiral wave pattern emerges. When the parameters are located in domain IV, both Hopf and Turing instability occur, and the stationary state of stripe-like pattern exists.

Turing instability is relevant not only in reaction-diffusion systems, but also in describing other dissipative structures, which can be understood in terms of diffusion-driven instability. In addition to the biological relevance of Turing systems, their ability to generate structure is of great interest from the point of view of physics. There are various physical systems that show similar phenomena, although the underlying mechanisms can be very different. Thus, most of the research in the field relies on experiments and numerical simulations justified by an analytical examination. In addition, in simulations one may study pattern formation under constraints that are beyond the reach of experiments and the numerical data is also easy to analyze.

In Ref. [2], it's indicated that the basic idea of diffusion-driven instability in a reaction-diffusion model can be understood in terms of an activator-inhibitor system. And a random increase of activator species (prey, N) has a positive effect on the creation rate of both activator and inhibitor (predator, P) species. In other words, random fluctuations may cause a nonuniform prey density. This elevated prey density has a positive effect both on prey and predator population growth rates. Following D. Alonso *et al* [2], we give the discussion to model(2). From Eqs.(2), we can obtain the following equations:

$$\frac{1}{N} \frac{\partial N}{\partial t} = r \left(1 - \frac{N}{K}\right) - \frac{\beta P}{B+N+wP}, \quad \frac{1}{P} \frac{\partial P}{\partial t} = \frac{\varepsilon \beta N}{B+N+wP} - \eta. \quad (10)$$

Similar to Ref. [2], the first equation in Eqs.(10) is a one-humped function of prey density, the numerical result can be found in [20], and prey growth rate can be increased by a higher local prey density at least in a range of parameter

values. On the other hand, the second equation in Eqs.(10), i.e., predator numerical response, is an ever-increasing function of N , and high prey density always has a positive influence on predator growth. More importantly, inhibitor species (predator, P) must diffuse faster than activator species (prey, N), for an increment in inhibitor species may have a negative effect on formation rate of both species. Thus, as random fluctuations increase local prey density over its equilibrium value, prey population undergoes an accelerated growth. Simultaneously, predator population also increases, but as predators diffuse faster than prey, they disperse away from the center of prey outbreaks. If relative diffusion (d_2/d_1) is large enough, prey growth rate will reach negative values and prey population will be driven by predators to a very low level in those regions. The final result is the formation of patches of high prey density surrounded by areas of low prey density. Predators follow the same pattern.

In Ref. [11], Neuhauser and Pacala formulated the Lotka-Volterra model as a spatial one. They found the striking result that the coexistence of patterns is actually harder to get in the spatial model than in the non-spatial one. One reason can be traced to how local interaction between individual members of the species are represented in the model. In this study, our results show that the predator-prey model with Beddington-DeAngelis-type functional response and reaction-diffusion (e.g., Eqs. 2) also represents rich spatial dynamics, such as spotted pattern, stripe-like pattern, coexistence of both stripe-like and spotted pattern, spiral pattern, etc. It will be useful for studying the dynamic complexity of ecosystems or physical systems. In Ref. [9], it is indicated that reaction-diffusion models provide a way to translate local assumptions about the movement, mortality, and reproduction of individuals into global conclusions about the persistence or extinction of populations and the coexistence of interacting species. They can be derived mechanistically via rescaling from models of individual movement which are based on random walks, i.e., small random perturbation of the stationary solution (N^*, P^*) of the spatially homogeneous model (2). Reaction-diffusion system, i.e., model (2), is spatially explicit and typically incorporate quantities such as dispersal rates, local growth rates, and carrying capacities as parameters which may vary with location or time.

More interesting, when the parameters are located in domain III, pure Hopf instability occurs, and the spiral wave pattern emerges (c.f., Fig. 5, Fig. 6(C)). To our knowledge, we haven't got any report about one system that has spotted, stripe-like and spiral pattern meantime. It's well known that spirals and curves are the most fascinating clusters to emerge from the predator-prey model. A spiral will form from a wave front when the rabbit line (which is leading the front) overlaps the pursuing line of predator. The prey on the extreme end of the line stop moving as there are no predator in their immediate vicinity. However the prey and the predator in the center of the line continue moving forward. This forms a small trail of prey at one (or both) ends of the front. These prey start breeding and the trailing line of prey thickens and attracts the attention of predator at the end of the fox line that turn towards this new source of prey. Thus a spiral forms with predator on the inside and prey on the outside. If the original overlap of prey occurs at both ends of the line a double spiral will form. Spirals can also form as a prey blob collapses after predator eat into it [23, 24]. Thus, reaction-diffusion system provides a good framework for studying questions about the ways that habitat geometry and the size or variation in vital parameters influence population dynamics.

On the other hand, one can see that although there is a small difference between the denominators of the functional responses of Michaelis-Menten-type and those of Beddington-DeAngelis-type, there is an enormous gap between them in the process of computations. The Turing bifurcation expression of Michaelis-Menten-type predator-prey system is simple [64], while from (9), one can see that the Turing bifurcation analysis requires huge-sized computations, so we have to obtain more help via computers.

In fact, computer aided analysis is useful for nonlinear analysis. And computers have played an important role throughout the history of ecology. Today, numerical simulations also play an important role in spatial ecology. There are some international mathematical softwares, such as **Matlab**, **Maple**, **Mathematica**, etc. We have finished all our symbolic computations in **Maple** and obtained our pattern snapshots (i.e., numerical simulations) in **Matlab** for **Maple** is more superior in symbolic computations while **Matlab** is more superior in numerical computations.

Acknowledgments This work was supported by the National Natural Science Foundation of China (10471040) and the Youth Science Foundation of Shanxi Province (20041004).

-
- [1] Abrams, P. A., Ginzburg, L. R., 2000. The nature of predation: prey dependent, ratio dependent or neither? *Trends Ecol. Evol.* 8, 337-341.
 - [2] Alonso, D., Bartumeus, F., Catalan, J., 2002. Mutual interference between predators can give rise to Turing spatial patterns, *Ecology* 83, 28-34.

- [3] Andrew M., Sergei P., Li, B.-L., 2006. Spatiotemporal complexity of patchy invasion in a predator-prey system with the Allee effect, *J.Theor. Biol.* 238, 18-35.
- [4] Arditi, R., Ginzburg, L. R., 1989. Coupling in predator-prey dynamics: Ratio-Dependence, *J. Theor. Biol.*139, 311-326.
- [5] Baumann, M., Gross, T., Feudel, U., 2007. Instabilities in spatially extended predator-prey systems: Spatio-temporal patterns in the neighborhood of Turing-Hopf bifurcations, *J. Theor. Biol.* 245, 220-229.
- [6] Beddington, J. R., 1975. Mutual interference between parasites or predators and its effect on searching efficiency, *J. Anim. Ecol.* 44, 331-340.
- [7] Berryman, A. A., 1992. The Origins and Evolution of Predator-Prey Theory, *Ecology* 73, 1530-1535.
- [8] Cantrell, R. S., Cosner, C., 2001. On the Dynamics of Predator-Prey Models with the Beddington-DeAngelis Functional Response, *J. Math. Anal. Appl.* 257, 206-222.
- [9] Cantrell, R., Cosner, C., 2003. *Spatial Ecology via Reaction-Diffusion Equations*, John Wiley & Sons, Ltd., Chichester, England.
- [10] Claudia, N., 2001. Mathematical Challenges in Spatial Ecology, *Notices of the American Mathematical Society* 47, 1304-1314.
- [11] Claudia N., Stephen W. P., 1999. An explicitly spatial version of the Lotka-Volterra model with interspecific competition, *Ann. Appl. Probab* 9, 1226-1259.
- [12] Cross, M. C., Hohenberg, P. C., 1993. Pattern formation outside of equilibrium, *Rev. Mod. Phys.* 65, 851.
- [13] Crowley P. H., and Martin, E. K., 1989. Functional responses and interference within and between year classes of a dragonfly population, *J. North Amer. Bent. Soc.* 8, 211-221.
- [14] Cui, J., Takeuchi, Y., 2006. Permanence, extinction and periodic solution of predator-prey system with Beddington-DeAngelis functional response, *J. Math. Anal. Appl.*317, 464-474.
- [15] DeAngelis, D. L., Goldstein, R. A., and Neill, R., 1975. A model for trophic interaction, *Ecology* 56, 881-892.
- [16] Dobromir T. ., Hristo V. K., 2005. Complete mathematical analysis of predator-prey models with linear prey growth and Beddington-DeAngelis functional response, *Appl. Math. Comp.* 162, 523-538.
- [17] Evelyn S., Thomas W., 2003. Pattern formation in a nonlinear model for animal coats, *J. Diff. Equa.* 191, 143-174.
- [18] Fan, M., Kuang, Y., 2004. Dynamics of a nonautonomous predator-prey system with the Beddington-DeAngelis functional response, *J. Math. Anal. Appl.* 295, 15-39.
- [19] Garvie, M. R., 2007. Finite-difference schemes for reaction-diffusion equations modelling predator-prey interactions in Matlab, *Bull. Math. Bio.* 69, 931-956.
- [20] Huisman, G., DeBoer R. J., 1997. A Formal Derivation of the “Beddington” Functional Response, *J. Theor. Biol.* 185, 389-400.
- [21] Gierer, A., Meinhardt, H., 1972. A theory of biological pattern formation, *Kybernetik* 12, 30-39.
- [22] Griffith, D. A., Peres-Neto, P. R., 2006. Spatial modeling in ecology: the flexibility of eigenfunction spatial analyses, *Ecology* 87, 2603-2613.
- [23] Gurney, W. S. C., Veitch, A. R., Cruickshank, I., McGeachin, G., 1998. Circles and spirals: population persistence in a spatially explicit predator-prey model, *Ecology* 79, 2516-2530.
- [24] Hawick, K., James, H., Scogings, C., 2006. A zoology of emergent life patterns in a predator-prey simulation model, Technical Note CSTN-015 and in Proc. IASTED International Conference on Modelling, Simulation and Optimization, September 2006, Gabarone, Botswana. 107-115.
- [25] Hassell, M. P., Varley, C. C., 1969. New inductive population model for insect parasites and its bearing on biological control, *Nature* 223, 1133-1177.
- [26] Holling, C. S., 1959. The components of predation as revealed by a study of small mammal predation of the European pine sawfly, *Can. Ento.* 91, 293-320.
- [27] Holling, C. S., 1959. Some characteristics of simple types of predation and parasitism, *Can. Ento.* 91, 385-395.
- [28] Hwang, T.-W., 2003. Global analysis of the predator-prey system with Beddington-DeAngelis functional response, *J. Math. Anal. Appl.* 281, 395-401.
- [29] Jost, C., 1998. Comparing predator-prey models qualitatively and quantitatively with ecological time-series data, PhD-Thesis, Institute National Agronomique, Paris-Grignon.
- [30] Jost, C., Arino, O., Arditi, R., 1999. About deterministic extinction in ratio-dependent predator-prey models, *Bull. Math. Biol.*61, 19-32.
- [31] Just, W., Bose, M., Bose, S., Engel, H., Schöll, E., 2001. Spatiotemporal dynamics near a supercritical Turing-Hopf bifurcation in a two-dimensional reaction-diffusion system, *Phys. Rev. E* 64, 026219.
- [32] Kar, T. K., and Pahari, U. K., 2007. Modelling and analysis of a prey-predator system with stage-structure and harvesting, *Nonl. Anal.: Real World Appl.* 8, 601-609.
- [33] Karen P., Maini, P. K., Nicholas, A.M., 2003. Pattern formation in spatially heterogeneous Turing reaction-diffusion models, *Phys. D* 181, 80-101.
- [34] Klausmeier, C. A., 1999. Regular and Irregular Patterns in Semiarid Vegetation, *Science* 284, 1826-1828.
- [35] Kuang, Y., Beretta, E., 1998. Global qualitative analysis of a ratio-dependent predator-prey system, *J. Math. Biol.*36, 389-406.
- [36] Lejeune, O., Tlidi, M., Couteron, P., 2002. Localized vegetation patches: A self-organized response to resource scarcity, *Phys. Rev. E* 66, 010901.
- [37] Leppänen, T., 2004. Computational studies of pattern formation in turing systems, Phd-thesis, Helsinki University of Technology, Finland.
- [38] Leppänen, T., Karttunen, M., Barrio, R. A., Kaski, K., 2004. Morphological transitions and bistability in Turing systems,

- Phys. Rev. E 70, 066202.
- [39] Levin, S. A., 1992. The Problem of Pattern and Scale in Ecology, *Ecology* 73, 1943-1967.
 - [40] Levin, S. A., Grenfell, B., Hastings, A., Perelson, A. S., 1997. Mathematical and Computational Challenges in Population Biology and Ecosystems Science, *Science* 275, 334-343.
 - [41] Levin, S. A., Segel, L. A., 1976. Hypothesis for origin of planktonic patchiness, *Nature* 259, 659.
 - [42] Li, Z., Wang, W., Wang, H., 2006. The dynamics of a Beddington-type system with impulsive control strategy, *Chaos, Solitons and Fractals* 29, 1229-1239.
 - [43] Liu, Q., Jin, Z., Liu, M., 2006. Spatial organization and evolution period of the epidemic model using cellular automata, *Phys. Rev. E* 74, 031110.
 - [44] Liu, Q., Jin, Z., 2007. Formation of spatial patterns in epidemic model with constant removal rate of the infectives, *J. Stat. Mech.* P05002.
 - [45] Liu, R. T., Liaw, S. S., and Maini, P. K., 2006. Two-stage Turing model for generating pigment patterns on the leopard and the jaguar, *Phys. Rev. E* 74, 011914.
 - [46] Liu, S., Edoardo B., 2006. A stage-structured predator-prey model of Beddington-Deangelis type, *SIAM J. Appl. Math.* 66, 1101-1129.
 - [47] Maini, P. K., 2004. Using mathematical models to help understand biological pattern formation, *Comp. Rend. Biol.* 327, 225-234.
 - [48] Maini, P. K., Baker, R. E., and Chuong, C., 2006. The Turing model comes of molecular age, *Science* 314, 1397-1398.
 - [49] Maionchi, D. O., Reis, S. F., Aguiar, M. A. M., 2006. Chaos and pattern formation in a spatial tritrophic food chain, *Ecol. Model.* 191, 291-303.
 - [50] Medvinsky, A., Petrovskii, S., Tikhonova, I., Malchow, H., Li, B-L., 2002. Spatiotemporal complexity of plankton and fish dynamics, *SIAM Review* 44, 311-370.
 - [51] Murray, J., 2003. *Mathematical Biology II: Spatial Models and Biomedical Applications*. Springer, Berlin.
 - [52] Ouyang, Q. Swinney, H. L., 1991. Transition from a uniform state to hexagonal and striped Turing patterns, *Nature* 352, 610-612.
 - [53] Pascual, M., 1993. Diffusion-induced chaos in a spatial predator-prey system, *Proc. Roy. Soc. Lond. B* 251, 1-7.
 - [54] Pascual, M., Roy, M., Franc, A., 2002. Simple temporal models for ecological systems with complex spatial patterns, *Ecol. Lett.* 5, 412-419.
 - [55] Ruan, S., Xiao, D., 2001. Global Analysis in a Predator-Prey System with Nonmonotonic Functional Response, *SIAM J. Appl. Math.* 61, 1445-1472.
 - [56] Segel, L. A., Jackson, J. L., 1972. Dissipative structure: An explanation and an ecological example, *J. Theor. Biol.* 37, 545-559.
 - [57] Seydel, R., 1994. *Practical bifurcation and stability analysis*, Springer, New York.
 - [58] Shuji I., Kunihiko K., 2006. Turing pattern with proportion preservation, *J. Theo. Ecol.* 238, 683-693.
 - [59] Skalski, G. T., Gilliam, J. F., 2001. Functional responses with predator interference: Viable alternatives to the Holling type II model, *Ecology* 82, 3083-3092.
 - [60] Arecchi, F. T., Stefano Boccaletti, and PierLuigi Ramazza, 1999. Pattern formation and competition in nonlinear optics, *Phys. Repo.* 318, 1-83.
 - [61] Turing, A. M., 1952. The chemical basis of morphogenesis, *Phil. Trans. R. Soc. London B* 237, 7-72.
 - [62] Vanag, V. K., Yang, L., Dolnik, M., Zhabotinsky, A. M., Epstein, I. R., 2000. Oscillatory cluster patterns in a homogeneous chemical system with global feedback, *Nature* 406, 389-391.
 - [63] Von Hardenberg, J., Meron, E., Shachak, M., Zarmi, Y., 2001. Diversity of Vegetation Patterns and Desertification, *Phys. Rev. Lett.* 87, 198101.
 - [64] Wang, W., Liu, Q., and Jin, Z., 2007. Spatiotemporal complexity of a ratio-dependent predator-prey system, *Phys. Rev. E* 75, 051913.
 - [65] Wang, W., Wang, H., Li, Z., 2007. The dynamic complexity of a three-species Beddington-type food chain with impulsive control strategy, *Chaos, Solitons and Fractals* 32, 1772-1785.
 - [66] Yang, L., Dolnik, M., Zhabotinsky, A. M., Epstein, I. R., 2002. Pattern formation arising from interactions between Turing and wave instabilities, *J. Chem. Phys.* 117, 7259-7265.
 - [67] Yang, L., Dolnik, M., Zhabotinsky, A. M., Epstein, I. R., 2002. Spatial Resonances and Superposition Patterns in a Reaction-Diffusion Model with Interacting Turing Modes, *Phys. Rev. Lett.* 88, 208303.
 - [68] Yang, L., Irving R. E., 2003. Oscillatory Turing Patterns in Reaction-Diffusion Systems with Two Coupled Layers, *Phys. Rev. Lett.* 90, 178303.
 - [69] Yang, L., Irving R. E., 2004. Symmetric, asymmetric, and antiphase Turing patterns in a model system with two identical coupled layers, *Phys. Rev. E* 69, 026211.
 - [70] Yang, L., Milos D., Anatol M. Z., Irving R. E., 2006. Turing patterns beyond hexagons and stripes, *Chaos* 16, 037114.

Spatiotemporal pattern formation of Beddington-DeAngelis-type predator-prey model

Weiming Wang* and Lei Zhang

Institute of Nonlinear Analysis, College of Mathematics and Information Science,

Wenzhou University, Wenzhou, Zhejiang, 325035 and

Department of Mathematics, North University of China, Taiyuan, Shan'xi 030051, P.R. China

Yakui Xue and Zhen Jin

Department of Mathematics, North University of China, Taiyuan, Shan'xi 030051, P.R. China

(Dated: September 5, 2021)

In this paper, we investigate the emergence of a predator-prey model with Beddington-DeAngelis-type functional response and reaction-diffusion. We derive the conditions for Hopf and Turing bifurcation on the spatial domain. Based on the stability and bifurcation analysis, we give the spatial pattern formation via numerical simulation, i.e., the evolution process of the model near the coexistence equilibrium point. We find that for the model we consider, pure Turing instability gives birth to the spotted pattern, pure Hopf instability gives birth to the spiral wave pattern, and both Hopf and Turing instability give birth to stripe-like pattern. Our results show that reaction-diffusion model is an appropriate tool for investigating fundamental mechanism of complex spatiotemporal dynamics. It will be useful for studying the dynamic complexity of ecosystems.

PACS numbers:

Keywords: Reaction-diffusion equations; Hopf bifurcation; Turing instability; Spatiotemporal pattern

Contents

1. Introduction	1
2. Stability and bifurcation analysis	3
3. Spatiotemporal pattern formation	6
4. Conclusions and remarks	10
References	12

1. INTRODUCTION

Mathematical models have played an important role throughout the history of ecology. Models in ecology serve a variety of purposes, which range from illustrating an idea to parameterizing a complex real-world situation. They are used to make general predictions, to guide management practices, and to provide a basis for the development of statistical tools and testable hypotheses [10, 40, 51].

A fundamental goal of theoretical ecology is to understand how the interactions of individual organisms with each other and with the environment determine the distribution of populations and the structure of communities [9]. As we know, our ecological environment is a huge and highly complex system. This complexity arises in part from the diversity of biological species, and also from the complexity of every individual organism [29, 30]. The dynamic behavior of predator-prey model has long been and will continue to be one of the dominant themes in both ecology and mathematical ecology due to its universal existence and importance [7, 35].

Before the 1970s, ecological population models typically used ordinary differential equations, seeking equilibria and analyzing stability. The early models provided important insights, such as when species can stably coexist and when predator and prey density oscillate over time [10].

*Electronic address: weimingwang2003@163.com

We live in a spatial world, and spatial patterns are ubiquitous in nature, which modify the temporal dynamics and stability properties of population density at a range of spatial scales, whose effects must be incorporated in temporal ecological models that do not represent space explicitly. And the spatial component of ecological interactions has been identified as an important factor in how ecological communities are shaped [10]. Empirical evidence suggests that the spatial scale and structure of the environment can influence population interactions and the composition of communities [9]. In recent decades, the role of spatial effects in maintaining biodiversity has received a great deal of attention in the literature on conservation [5, 22, 39, 43, 49, 50, 51, 64].

The past investigations have revealed that spatial inhomogeneities like the inhomogeneous distribution of nutrients as well as interactions on spatial scales like migration can have an important impact on the dynamics of ecological populations [50, 51]. In particular it has been shown that spatial inhomogeneities promote the persistence of ecological populations, play an important role in speciation and stabilize population levels [5]. Spatial ecology today is still dominated by theoretical investigations, and empirical studies that explore the role of space are becoming more common due to technological advances that allow the recording of exact spatial locations [10].

In 1952, Alan Turing, one of the key scientists of 20th century, mathematically showed that a system of coupled reaction-diffusion equations could give rise to spatial concentration patterns of a fixed characteristic length from an arbitrary initial configuration due to diffusion-driven instability [61]. The work by Turing belongs to the field of pattern formation, a subfield of mathematical biology. Pattern formation in nonlinear complex systems is one of the central problems of the natural, social, and technological sciences. The occurrence of multiple steady states and transitions from one to another after critical fluctuations, the phenomena of excitability, oscillations, waves and the emergence of macroscopic order from microscopic interactions in various nonlinear nonequilibrium systems in nature and society have been the subject of many theoretical and experimental studies [50]. It has been qualitatively shown that Turing models can indeed imitate biological patterns [37].

The study of biological pattern formation has gained popularity since the 1970s, and Segel and Jackson [56] were the first to apply Turing's ideas to a problem in population dynamics: the dissipative instability in the predator-prey interaction of phytoplankton and herbivorous copepods with higher herbivore motility. At the same time, Gierer and Meinhardt [21] gave a biologically justified formulation of a Turing model and studied its properties by employing numerical simulations. Levin and Segel [41] suggested this scenario of spatial pattern formation was a possible origin of planktonic patchiness.

Spatial patterns and aggregated population distributions are common in nature and in a variety of spatiotemporal models with local ecological interactions [54]. And the understanding of patterns and mechanism of species spatial dispersal is an issue of current interest in conservation biology and ecology [3, 39, 50]. It arises from many ecological applications, and in particular, plays a major role in connection to biological invasion and epidemic spread and so on [3, 5, 10, 19, 39, 43, 47, 48, 50, 51]. The field of research on pattern formation modeled by reaction-diffusion systems, which provides a general theoretical framework for describing pattern formation in systems from many diverse disciplines including biology [9, 34, 36, 39, 45, 50, 53, 54, 58, 63, 64], chemistry [17, 33, 52, 62, 66, 67, 68, 69, 70], physics [12, 31, 38, 60], epidemiology [43, 44] and so on, seems to be a new increasingly interesting area, particularly during the last decade.

In general, a classical predator-prey model can be written as the form [2, 4]:

$$\dot{N} = Nf(N) - Pg(N, P), \quad \dot{P} = h[g(N, P), P]P.$$

where N and P are prey and predator densities, respectively, $f(N)$ the prey growth rate, $g(N, P)$ the functional response, e.g., the prey consumption rate by an average single predator, and $h[g(N, P), P]$ the per capita growth rate of predators (also known as the "predator numerical response"), which obviously increases with the prey consumption rate. The most widely accepted assumption for the numerical response is the linear one [2]:

$$h[g(N, P), P] = \varepsilon g(N, P) - \eta$$

where η is a per capita predator death rate and ε the conversion efficiency of food into offspring.

In population dynamics, a functional response $g(N, P)$ of the predator to the prey density refers to the change in the density of prey attached per unit time per predator as the prey density changes [1, 55]. There have been several famous functional response types: Holling types I–III [26, 27]; Hassell-Varley type [25]; Beddington-DeAngelis type by Beddington [6] and DeAngelis *et al* [15] independently; the Crowley-Martin type [13]; and the recent well-known ratio-dependence type by Arditi and Ginzburg [4] later studied by Kuang and Beretta [35]. Of them, the Holling type I-III is labeled "prey-dependent" and other types that consider the interference among predators are labeled "predator-dependent" [4].

In our previous work [64], we studied the spatiotemporal complexity of a ratio-dependent predator-prey model with Michaelis-Menten-type functional response. Compare Michaelis-Menten-type functional response

$$g(N, P) = \frac{\alpha N}{P + \alpha h N}$$

(α, h are positive constants, α capture rate and h handling time) with Beddington-DeAngelis-type functional response

$$g(N, P) = \frac{\beta N}{B + N + wP} \quad (1)$$

(β, B are positive constants, β a maximum consumption rate, B a saturation constant, w a predator interference parameter, a constant. $w < 0$ is the case where predators benefit from cofeeding). Some scholars [2, 46, 59] indicate that where there is a small difference between the denominators, there is a world between them from the biological point.

If predators do not waste time interacting with one another or if their attacks are always successful and instantaneous, i.e., $w = 0$ in (1), then a Holling type II functional response is obtained:

$$g(N) = \frac{\beta N}{B + N}.$$

If $B = 0$ in (1), the Michaelis-Menten-type functional response is obtained.

Furthermore, in [59], by comparing the statistical evidence from nineteen categories of predator-prey systems with three predator-dependent functional responses, Skalski and Gilliam pointed out that the predator-dependent functional responses could provide better descriptions of predator feeding over a range of predator-prey abundance, and in some cases, the Beddington-DeAngelis-type functional response performed even better [46].

Some progress has been seen in the study of predator-prey model with Beddington-DeAngelis-type functional response [2, 8, 14, 16, 18, 20, 28, 29, 32, 42, 46, 65]. However, the research on considering reaction-diffusion to such a model, to our knowledge, seems rare.

In this paper, we report a study of Turing pattern formation in a two-species reaction-diffusion predator-prey model with Beddington-DeAngelis-type functional response. In the next section we give a brief stability and bifurcation analysis of the model. Then, we present and discuss the results of numerical simulations, which is followed by the last section, i.e., conclusions and remarks.

2. STABILITY AND BIFURCATION ANALYSIS

In this paper, we mainly focus on the following predator-prey model with Beddington-DeAngelis-type functional response and reaction-diffusion:

$$\frac{\partial N}{\partial t} = r \left(1 - \frac{N}{K}\right) N - \frac{\beta N}{B + N + wP} P + d_1 \nabla^2 N, \quad \frac{\partial P}{\partial t} = \frac{\varepsilon \beta N}{B + N + wP} P - \eta P + d_2 \nabla^2 P. \quad (2)$$

where t denotes time and N, P stand for prey and predator density, respectively. All parameters are positive constants, r standing for maximum per capita growth rate of the prey, β capture rate, η predator death rate, w a predator interference parameter and K carrying capacity, which is the nonzero equilibrium population size. The diffusion coefficients are denoted by d_1 and d_2 , respectively. $\nabla^2 = \frac{\partial}{\partial x^2} + \frac{\partial}{\partial y^2}$ is the usual Laplacian operator in two-dimensional space.

The first step in analyzing the model is to determine the equilibria (stationary states) of the non-spatial model obtained by setting space derivatives equal to zero, i.e.,

$$r \left(1 - \frac{N}{K}\right) N - \frac{\beta N}{B + N + wP} P = 0, \quad \frac{\varepsilon \beta N}{B + N + wP} P - \eta P = 0. \quad (3)$$

In fact, physically, an equilibrium represents a situation without “life”. It may mean no motion of a pendulum, no reaction in a reactor, no nerve activity, no flutter of an airfoil, no laser operation, or no circadian rhythms of biological clocks [57]. And at each equilibrium point, the movement of the population dynamics vanishes.

Eqs.(3) has at most three equilibria, which correspond to spatially homogeneous equilibria of the full model, Eq.(2), in the positive quadrant:

(i) $(0, 0)$ (total extinct) is a saddle point.

(ii) $(K, 0)$ (extinct of the predator, or prey-only) is a stable node if $\varepsilon\beta < \eta$ or if $\varepsilon\beta > \eta$ and $K < -\frac{\eta B}{-\varepsilon\beta + \eta}$; a saddle if $\varepsilon\beta < \eta$ and $K > -\frac{\eta B}{-\varepsilon\beta + \eta}$; a saddle-node if $\varepsilon\beta < \eta$ and $K = -\frac{\eta B}{-\varepsilon\beta + \eta}$.

(iii) a nontrivial stationary state (N^*, P^*) (coexistence of prey and predator), where

$$N^* = \frac{1}{2rw\varepsilon} \left(K(rw\varepsilon - \varepsilon\beta + \eta) + \sqrt{K^2(rw\varepsilon - \varepsilon\beta + \eta)^2 + 4rKw\varepsilon\eta B} \right),$$

$$P^* = \frac{(\beta\varepsilon - \eta)}{w\eta} N^* - \frac{B}{w}.$$

To perform a linear stability analysis, we linearize the dynamic system 2 around the equilibrium point (N^*, P^*) for small space- and time-dependent fluctuations and expand them in Fourier space

$$N(\vec{x}, t) \sim N^* e^{\lambda t} e^{i\vec{k}\cdot\vec{x}}, \quad P(\vec{x}, t) \sim P^* e^{\lambda t} e^{i\vec{k}\cdot\vec{x}},$$

and obtain the characteristic equation

$$|A - k^2 D - \lambda I| = 0, \quad (4)$$

where $D = \text{diag}(d_1, d_2)$ and the Jacobian matrix A is given by

$$A = \begin{pmatrix} \partial_n f & \partial_p f \\ \partial_n g & \partial_p g \end{pmatrix}_{(N^*, P^*)} = \begin{pmatrix} f_n & f_p \\ g_n & g_p \end{pmatrix}.$$

Now Eq.(4) can be solved, yielding the so called characteristic polynomial of the original problem (2):

$$\lambda^2 - \text{tr}_k \lambda + \Delta_k = 0, \quad (5)$$

where

$$\text{tr}_k = f_n + g_p - k^2(d_1 + d_2) = \text{tr}_0 - k^2(d_1 + d_2),$$

$$\Delta_k = f_n g_p - f_p g_n - k^2(f_n d_2 + g_p d_1) + k^4 d_1 d_2 = \Delta_0 - k^2(f_n d_2 + g_p d_1) + k^4 d_1 d_2.$$

The roots of Eq.(5) yield the dispersion relation

$$\lambda(k) = \frac{1}{2} \left(\text{tr}_k \pm \sqrt{\text{tr}_k^2 - 4\Delta_k} \right). \quad (6)$$

We know that one type of instability (or bifurcation) will break one type of symmetry of a system, i.e., in the bifurcation point, two equilibrium states intersect and exchange their stability. Biologically speaking, this bifurcation corresponds to a smooth transition between equilibrium states. The Hopf bifurcation is space-independent and it breaks the temporal symmetry of a system and gives rise to oscillations that are uniform in space and periodic in time. The Turing bifurcation breaks spatial symmetry, leading to the formation of patterns that are stationary in time and oscillatory in space.

The Hopf instability or bifurcation is an important instability in reaction-diffusion systems for which the conditions result in a stable limit cycle (oscillations). In terms of the linearized problem (Eq.4) the onset of Hopf instability corresponds to the case, when a pair of imaginary eigenvalues cross the real axis from the negative to the positive side. The Hopf bifurcation of an equilibrium state is reflected by a transition between stationary and periodic behavior. If the system is in a stable equilibrium before the bifurcation, the stability is lost at the bifurcation point. As a result the system abundance of species start to oscillate periodically. And this situation occurs only when the diffusion vanishes. Mathematically speaking, the Hopf bifurcation occurs when $\text{Im}(\lambda(k)) \neq 0$, $\text{Re}(\lambda(k)) = 0$ at $k = 0$. Then we can get the critical value of the transition, Hopf bifurcation parameter— K , equals

$$K_H = \frac{B(w\varepsilon\eta - \beta\varepsilon - \eta)^2}{(w\varepsilon - 1)(\eta^2 - \beta^2\varepsilon^2 + rw\varepsilon^2\beta + \varepsilon^2\beta w\eta - w\varepsilon\eta^2)} \quad (7)$$

At the Hopf bifurcation threshold, the temporal symmetry of the system is broken and gives rise to uniform oscillations in space and periodic oscillations in time with the frequency

$$\omega_H = \text{Im}(\lambda(k)) = \sqrt{\Delta_0},$$

where

$$\Delta_0 = -\frac{\left(K(\eta-\beta\varepsilon)(K(rw\varepsilon-\beta\varepsilon+\eta)^2+\eta\delta-\beta\delta\varepsilon+4rw\varepsilon\eta B+r\delta\varepsilon w)+2r\delta\eta B\varepsilon w\right)\eta}{\beta K\varepsilon^2 w(rKw\varepsilon-\beta K\varepsilon+K\eta+\delta)},$$

and

$$\delta = \left(r^2 K^2 w^2 \varepsilon^2 - 2 r K^2 w \varepsilon^2 \beta + 2 r K^2 w \varepsilon \eta + \beta^2 K^2 \varepsilon^2 - 2 \beta K^2 \varepsilon \eta + K^2 \eta^2 + 4 r w \varepsilon K \eta B\right)^{1/2}.$$

The corresponding wavelength is

$$\lambda_H = \frac{2\pi}{\omega_H} = \frac{2\pi}{\sqrt{\Delta_0}}.$$

The Turing instability is not dependent upon the geometry of the system but only upon the reaction rates and diffusion. And it cannot be expected when the diffusion term is absent and it can occur only when the activator (e.g., N) diffuses more slowly than the inhibitor (e.g., P). Linear analysis above shows that the necessary conditions for yielding Turing patterns are given by

$$f_n + g_p < 0, \quad f_n g_p - f_p g_n > 0, \quad d_2 g_p + d_1 f_n > 0, \quad (d_2 f_n + d_1 g_p)^2 > 4 d_1 d_2 (f_n g_p - f_p g_n).$$

Mathematically speaking, as $d_1 \ll d_2$, the Turing bifurcation occurs when

$$\text{Im}(\lambda(k)) = 0, \quad \text{Re}(\lambda(k)) = 0 \text{ at } k = k_T \neq 0,$$

and the wavenumber k_T satisfies $k_T^2 = \sqrt{\frac{\Delta_0}{d_1 d_2}}$. At the Turing bifurcation threshold, the spatial symmetry of the system is broken and the patterns are stationary in time and oscillatory in space with the corresponding wavelength

$$\lambda_T = \frac{2\pi}{k_T}. \quad (8)$$

And the critical value of Turing bifurcation parameter K takes the following form:

$$K_T = \frac{F_1 A + F_2}{G_1 A + G_2}, \quad (9)$$

where

$$\begin{aligned} A &= (-\eta d_1 (\varepsilon \beta - \eta) (-\varepsilon d_2 \beta - \eta d_2 + \varepsilon w \eta d_1))^2 (-\varepsilon \eta d_1 r w - \varepsilon \eta d_1 \beta + \varepsilon r^2 d_2 w - \varepsilon r d_2 \beta + d_1 \eta^2 - r d_2 \eta)^{1/2}, \\ F_1 &= -(\eta^2 (d_1 \varepsilon w - d_2)^2 + \varepsilon d_2 \beta (\varepsilon d_2 \beta + 2 \eta d_2 + 6 \varepsilon w \eta d_1))^2 ((-2 \varepsilon^2 \beta w d_2 (2 w \varepsilon \eta^2 d_1 d_2 - 4 w \varepsilon^2 \eta d_1 d_2 \beta - \eta^2 d_1^2 \varepsilon^2 w^2 \\ &\quad + \beta^2 d_2^2 \varepsilon^2 - d_2^2 \eta^2) r) + 2 \varepsilon d_2 \beta (\varepsilon \beta - \eta) (\varepsilon^2 (d_2 \beta + w \eta d_1)^2 + \eta d_2 (\eta d_2 - 2 \varepsilon w \eta d_1 + 2 \varepsilon d_2 \beta))) r B, \\ F_2 &= -(\eta^2 (d_1 \varepsilon w - d_2)^2 + \varepsilon d_2 \beta (\varepsilon d_2 \beta + 2 \eta d_2 + 6 \varepsilon w \eta d_1))^2 (\eta \beta \varepsilon^2 w d_2 (\varepsilon d_2 \beta + \eta d_2 - \varepsilon w \eta d_1) (\varepsilon^3 d_1 w (3 d_2 \beta + w \eta d_1)^2 \\ &\quad + d_2^3 (\eta + \varepsilon \beta)^2 - \varepsilon d_1 \eta^2 w d_2 (d_1 \varepsilon w + d_2)) r^2 - \eta (\varepsilon \beta - \eta) (\varepsilon d_2 \beta + \eta d_2 - \varepsilon w \eta d_1) (\varepsilon^4 \eta^3 w^4 d_1^4 + \varepsilon^3 \eta^2 w^3 d_2 (-4 \eta \\ &\quad + 9 \varepsilon \beta) d_1^3 + 3 \varepsilon^2 \eta w^2 d_2^2 (-5 \eta \varepsilon \beta + 2 \eta^2 + 9 \varepsilon^2 \beta^2) d_1^2 + \varepsilon w d_2^3 (11 \varepsilon \beta - 4 \eta) (\eta + \varepsilon \beta)^2 d_1 + d_2^4 (\eta + \varepsilon \beta)^3) r \\ &\quad + 2 \eta \beta d_1 \varepsilon d_2 (\varepsilon \beta - \eta)^2 (\varepsilon d_2 \beta + \eta d_2 - \varepsilon w \eta d_1) (\varepsilon^2 (d_2 \beta + w \eta d_1)^2 + \eta d_2 (\eta d_2 - 2 \varepsilon w \eta d_1 + 2 \varepsilon d_2 \beta))) r B, \\ G_1 &= G_{11} G_{12}, \\ G_{11} &= 4 \varepsilon d_2 \beta (-(\varepsilon^2 \beta d_2 (d_2 \beta - 4 w \eta d_1) - \eta^2 (d_1 \varepsilon w - d_2)^2) w \varepsilon r + (\varepsilon \beta - \eta) (\varepsilon^2 (d_2 \beta + w \eta d_1)^2 + \eta d_2 (\eta d_2 - 2 \varepsilon w \eta d_1 \\ &\quad + 2 \varepsilon d_2 \beta))), \\ G_{12} &= (\varepsilon^3 d_1 w (3 d_2 \beta + w \eta d_1)^2 + d_2^3 (\eta + \varepsilon \beta)^2 - \varepsilon d_1 \eta^2 w d_2 (d_1 \varepsilon w + d_2)) d_2 w \beta \varepsilon^2 r^2 - (\varepsilon \beta - \eta) (\varepsilon^3 d_2^3 (d_2 + 11 d_1 \varepsilon w) \beta^3 \\ &\quad + 3 d_2^2 \eta \varepsilon^2 (3 d_1 \varepsilon w + d_2)^2 \beta^2 + 3 \varepsilon \eta^2 d_2 (3 d_1 \varepsilon w + d_2) (d_1 \varepsilon w - d_2)^2 \beta + \eta^3 (d_1 \varepsilon w - d_2)^4) r + 2 \varepsilon \beta d_1 d_2 (\varepsilon \beta - \eta)^2 \\ &\quad (\varepsilon^2 (d_2 \beta + w \eta d_1)^2 + \eta d_2 (\eta d_2 - 2 \varepsilon w \eta d_1 + 2 \varepsilon d_2 \beta)), \end{aligned}$$

$$\begin{aligned}
G_2 &= G_{21}G_{22}, \\
G_{21} &= \varepsilon d_2\beta + \eta d_2 - \varepsilon w\eta d_1, \\
G_{22} &= g_0 + g_1r + g_2r^2 + g_3r^3 + g_4r^4, \\
g_0 &= 8\varepsilon^2\beta^2\eta d_1^2d_2^2(\varepsilon\beta - \eta)^4(\varepsilon^2(d_2\beta + w\eta d_1)^2 - 2\varepsilon d_1\eta^2wd_2 + d_2^2\eta^2 + 2\beta\varepsilon\eta d_2^2)^2, \\
g_1 &= 4\varepsilon\beta d_1d_2(\varepsilon\beta - \eta)^3(\varepsilon^2(d_2\beta + w\eta d_1)^2 - 2\varepsilon d_1\eta^2wd_2 + d_2^2\eta^2 + 2\beta\varepsilon\eta d_2^2)((d_1\varepsilon w - d_2)^4\eta^4 - 2\varepsilon\beta d_2(3d_1\varepsilon w + d_2) \\
&\quad (d_1\varepsilon w - d_2)^2\eta^3 - 16\varepsilon^3\beta^2d_1wd_2^2(d_1\varepsilon w + d_2)\eta^2 - 2\varepsilon^3d_2^3\beta^3(-d_2 + 5d_1\varepsilon w)\eta + d_2^4\varepsilon^4\beta^4), \\
g_2 &= (\varepsilon\beta - \eta)^2((d_1\varepsilon w - d_2)^8\eta^7 + 6\varepsilon\beta d_2(3d_1\varepsilon w + d_2)(d_1\varepsilon w - d_2)^6\eta^6 + \beta^2d_2^2\varepsilon^2(151\varepsilon^2w^2d_1^2 + 106\varepsilon d_1wd_2 + 15d_2^2) \\
&\quad (d_1\varepsilon w - d_2)^4\eta^5 + 4\varepsilon^3d_2^3\beta^3(156\varepsilon^3d_1^3w^3 + 133\varepsilon^2w^2d_1^2d_2 + 58wd_1\varepsilon d_2^2 + 5d_2^3)(d_1\varepsilon w - d_2)^2\eta^4 + d_2^4\varepsilon^4\beta^4(3d_1\varepsilon w \\
&\quad + d_2)(389\varepsilon^3d_1^3w^3 + 117\varepsilon^2w^2d_1^2d_2 + 183wd_1\varepsilon d_2^2 + 15d_2^3)\eta^3 + 2\varepsilon^5\beta^5d_2^5(357\varepsilon^3d_1^3w^3 + 297\varepsilon^2w^2d_1^2d_2 \\
&\quad + 47wd_1\varepsilon d_2^2 + 3d_2^3)\eta^2 + \varepsilon^6\beta^6d_2^6(153\varepsilon^2w^2d_1^2 + d_2^2 - 10\varepsilon d_1wd_2)\eta - 12\varepsilon^8\beta^7wd_1d_2^7), \\
g_3 &= -2\varepsilon^2\beta wd_2(\varepsilon\beta - \eta)((d_1\varepsilon w + d_2)(d_1\varepsilon w - d_2)^6\eta^6 + \varepsilon\beta d_2(13\varepsilon^2w^2d_1^2 + 6\varepsilon d_1wd_2 + 5d_2^2)(d_1\varepsilon w - d_2)^4\eta^5 \\
&\quad + 2\beta^2d_2^2\varepsilon^2(38\varepsilon^3d_1^3w^3 + \varepsilon^2w^2d_1^2d_2 + 20wd_1\varepsilon d_2^2 + 5d_2^3)(d_1\varepsilon w - d_2)^2\eta^4 + 2\varepsilon^3\beta^3d_2^3(5d_2^4 + 117\varepsilon^4w^4d_1^4 \\
&\quad + 44\varepsilon d_1wd_2^3 + 14d_2^2d_1^2w^2\varepsilon^2 - 52d_2d_1^3w^3\varepsilon^3)\eta^3 + d_2^4\varepsilon^4\beta^4(227\varepsilon^2w^2d_1^2d_2 + 329\varepsilon^3d_1^3w^3 + 79wd_1\varepsilon d_2^2 \\
&\quad + 5d_2^3)\eta^2 + \varepsilon^5\beta^5d_2^5(14\varepsilon d_1wd_2 + d_2^2 + 121\varepsilon^2w^2d_1^2)\eta - 6\varepsilon^7d_1wd_2^6\beta^6), \\
g_4 &= \varepsilon^4\beta^2w^2d_2^2((\varepsilon^2w^2d_1^2 + 6\varepsilon d_1wd_2 + d_2^2)(wd_1\varepsilon - d_2)^4\eta^5 + 4\varepsilon\beta d_2(2\varepsilon^3d_1^3w^3 + 13\varepsilon^2w^2d_1^2d_2 + d_2^3)(wd_1\varepsilon - d_2)^2\eta^4 \\
&\quad + 2\beta^2d_2^2\varepsilon^2(3d_2^4 + 52d_2d_1^3w^3\varepsilon^3 - 6d_2^2d_1^2w^2\varepsilon^2 + 4\varepsilon d_1wd_2^3 + 11\varepsilon^4w^4d_1^4)\eta^3 + 4\varepsilon^3\beta^3d_2^3(-9\varepsilon^2w^2d_1^2d_2 + d_2^3 \\
&\quad + 13\varepsilon^3d_1^3w^3 + 11wd_1\varepsilon d_2^2)\eta^2 + d_2^4\varepsilon^4\beta^4(113\varepsilon^2w^2d_1^2 + d_2^2 + 22\varepsilon d_1wd_2)\eta - 4d_2^5\varepsilon^6wd_1\beta^5),
\end{aligned}$$

In the following, linear stability analysis yields the bifurcation diagram with $r = 0.5$, $\varepsilon = 1$, $\beta = 0.6$, $B = 0.4$, $\eta = 0.25$, $w = 0.4$, $d_2 = 1$ shown in Fig. 1(A).

The Hopf bifurcation line and the Turing bifurcation curve separate the parametric space into four distinct domains. In domain I, located below all two bifurcation lines, the steady state is the only stable solution of the system. Domain II is the region of pure Turing instability, while domain III is the region of pure Hopf instability. In domain IV, which is located above all two bifurcation lines, both Hopf and Turing instability occur.

To see the relation between the real and the imaginary parts of the eigenvalue $\lambda(k)$, we plot in Fig. 1(B)–(F) the real and the imaginary parts of the eigenvalue at different K with $r = 0.5$, $\varepsilon = 1$, $\beta = 0.6$, $B = 0.4$, $\eta = 0.25$, $w = 0.4$, $d_1 = 0.01$ and $d_2 = 1$ for the system 2.

From the definition of Hopf and Turing bifurcation, we know that the relation between the real, the imaginary parts of the eigenvalue $\lambda(k)$ determine the bifurcation type. The relation between $\text{Re}(\lambda(k))$, $\text{Im}(\lambda(k))$ and k are shown in figure 1(B)–(F). Figure 1(B) illustrate the case of parameter locate in domain I in figure 1(A), $K = 2.131712170$, the critical value of Turing bifurcation, in this case, $\text{Re}(\lambda(k)) > 0$ at $k = 0$ while $\text{Im}(\lambda(k)) \neq 0$. In figure 1(C)(D), $K = 2.2$ and $K = 2.6$, the parameter locate in domain II, the pure Turing instability occurs, one can see that at $k = 0$, $\text{Re}(\lambda(k)) = 0$, $\text{Im}(\lambda(k)) \neq 0$. Figure 1(E), $K = 2.631578947$, the critical value of Hopf bifurcation, in this case, $\text{Re}(\lambda(k)) = 0$ at $k = 0$ while $\text{Im}(\lambda(k)) \neq 0$. When $K = 3.0$, parameter locate in domain IV, figure 1(F) indicate that at $k = 0$, $\text{Re}(\lambda(k)) > 0$, $\text{Im}(\lambda(k)) \neq 0$.

3. SPATIOTEMPORAL PATTERN FORMATION

In this section, we perform extensive numerical simulations of the spatially extended model (2) in two-dimensional spaces, and the qualitative results are shown here. All our numerical simulations employ the periodic Neumann (zero-flux) boundary conditions with a system size of 200×200 space units and $r = 0.5$, $\varepsilon = 1$, $\beta = 0.6$, $B = 0.4$, $\eta = 0.25$, $w = 0.4$, $d_1 = 0.01$ and $d_2 = 1$. The Eq.2 are solved numerically in two-dimensional space using a finite difference approximation for the spatial derivatives and an explicit Euler method for the time integration with a time stepsize of $\Delta t = 0.01$ and space stepsize (lattice constant) $\Delta h = 0.25$ (see, for details, [19]). The scale of the space and time are average to the Euler method. The initial density distribution corresponds to random perturbations around the stationary state (N^*, P^*) in model (2) with a variance significantly lower than the amplitude of the final patterns, which seems to be more general from the biological point of view. When the system reached a stable state

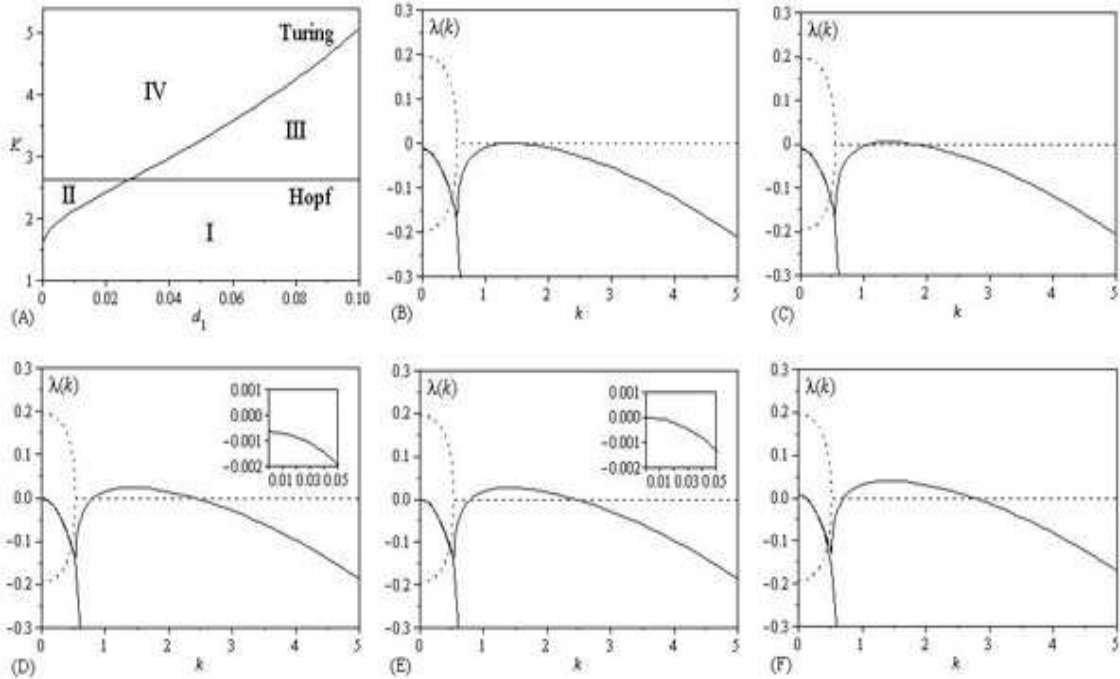


FIG. 1: (A) $K - d_1$ Bifurcation diagram for the model 2 with $r = 0.5$, $\varepsilon = 1$, $\beta = 0.6$, $B = 0.4$, $\eta = 0.25$, $w = 0.4$ and $d_2 = 1$. Hopf and Turing bifurcation lines separate the parameter space into four domains. And the Hopf-Turing bifurcation point is $(d_1, K) = (0.02742, 2.63158)$. In (B)—(F), $\text{Re}(\lambda(k))$ and $\text{Im}(\lambda(k))$ are shown by solid curves and dotted curves, respectively. The other parameters are: $d_1 = 0.01$, the bifurcation parameter K : (B) 2.131712170, the critical value of K_T ; (C) 2.2; (D) 2.6; (E) 2.631578947 the critical value of K_H ; (F) 3.0.

(stationary or oscillatory), we took a snapshot with yellow levels linearly proportional to the free species density and red corresponding to high while blue corresponding to low.

In the numerical simulations, different types of dynamics are observed and we have found that the distributions of predator and prey are always of the same type. Consequently, we can restrict our analysis of pattern formation to one distribution. In this section, we show the distribution of prey, for instance.

Fig. 2 shows the evolution of the spatial pattern of prey at 0, 10000, 200000 and 300000 iterations, with random small perturbation of the stationary solution $(N^*, P^*) = (0.5094, 0.7829)$ of the spatially homogeneous systems when $K = 2.2$, located in domain II, slightly more than the Turing bifurcation threshold $K_T = 2.1317$ and less than the Hopf bifurcation threshold $K_H = 2.6316$. In this case, one can see that for model 2, the random initial distribution (c.f., Fig. 2(A)) leads to the formation of a regular macroscopic spotted pattern which prevails over the whole domain at last, and the dynamics of the system does not undergo any further changes (c.f., Fig. 2(D)).

Fig. 3 shows the evolution of the spatial pattern of prey at 0, 10000, 30000 and 100000 iterations when $K = 2.6$ which is more than K_T and slightly less than K_H . Although the dynamics of the system starts from the stationary solution $(N^*, P^*) = (0.5252, 0.8382)$, there is an essential difference in the case above. From the snapshots, one can see that the steady state of spotted pattern and the stripe-like pattern coexist (c.f., Fig. 3(D)).

In Fig. 4, $K_H < K = 3.0$, i.e., parameters in domain IV, both Hopf and Turing instability occur. In this case, $(N^*, P^*) = (0.5380, 0.8831)$. One can see that the evolution of the spatial pattern of prey at 0, 20000, 50000 and 100000 iterations. After the spatial chaos patterns (c.f., Fig. 4(B)), a regular stationary stripe-like spatial state emerges (c.f., Fig. 4(D)).

When $K = 2.65$, $d_1 = 0.04$, i.e., parameters in domain III (c.f., Fig. 1(A)), pure Hopf instability occurs. As an example, the formation of a regular macroscopic two-dimensional spatial pattern, the spiral pattern, is shown in Fig. 5 with a system size of 400×400 space units. One can see that for model 2, the random initial distribution around the steady state $(N^*, P^*) = (0.5270, 0.8443)$, a unstable focus of model 2, leads to the formation of the spiral pattern in the domain (c.f., Fig. 5(D)). In other words, in this situation, spatially uniform steady-state predator-prey coexistence is no longer. Small random fluctuations will be strongly amplified by diffusion, leading to nonuniform population distributions. From the analysis in section II, we find with these parameters in domain III, the pattern formation, i.e., the spiral pattern, arises from pure Hopf instability. In order to make it clearer, in Fig. 6, we show

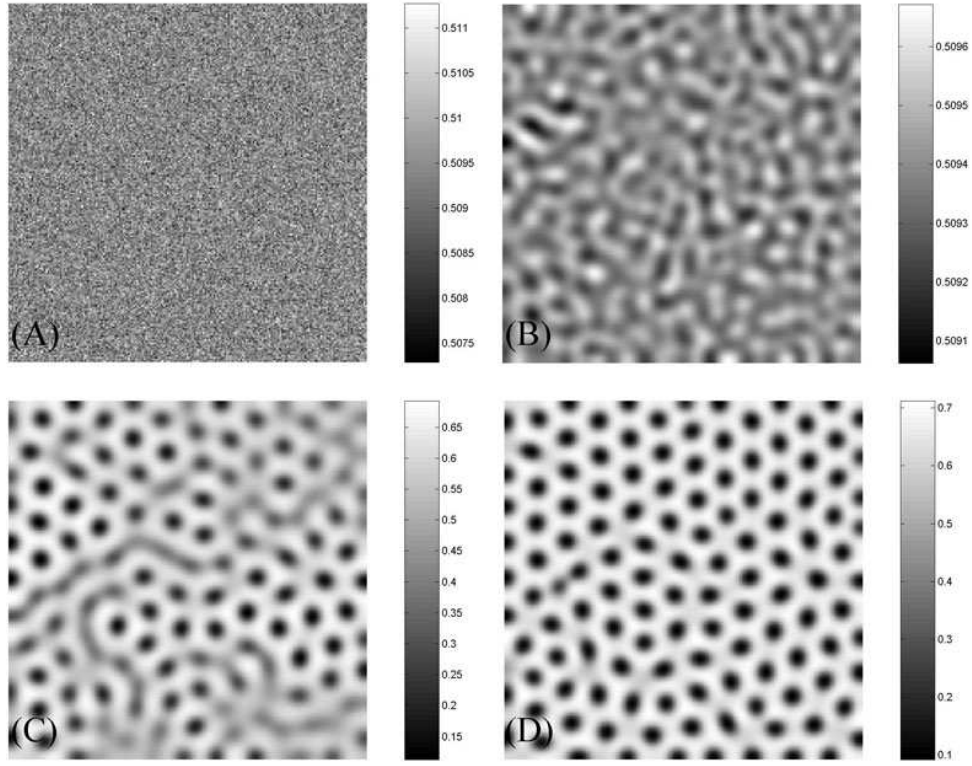


FIG. 2: Dynamics of the time evolution of the prey of model 2 with $d_1 = 0.01$, $K_T < K = 2.2 < K_H$. (A) 0 iteration, (B) 10000 iterations, (C) 200000 iterations, (D) 300000 iterations.

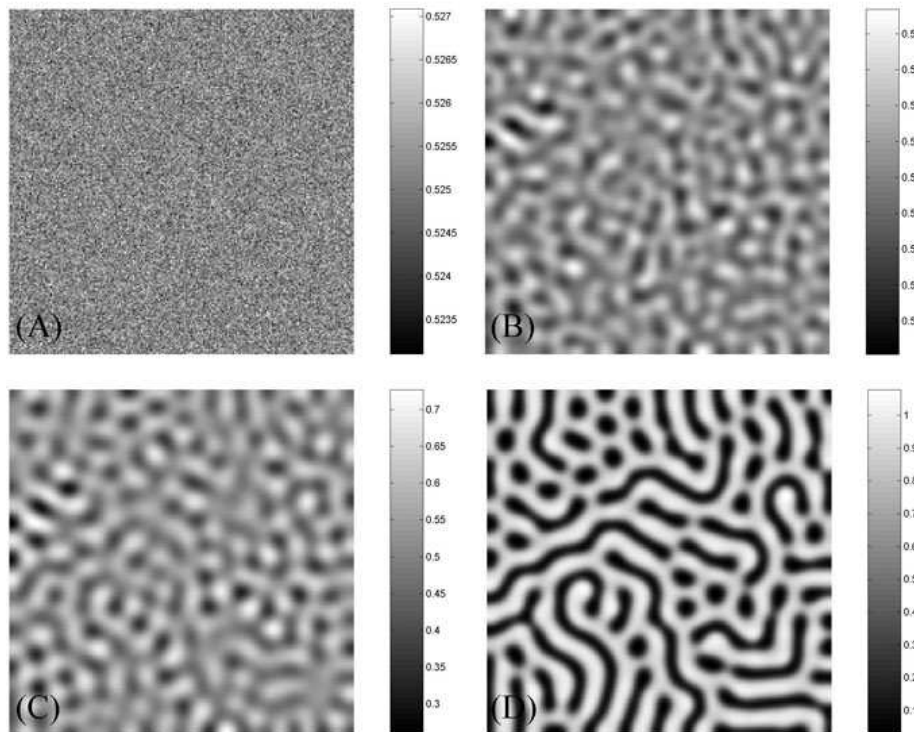


FIG. 3: Dynamics of the time evolution of the prey of model 2 with $d_1 = 0.01$, $K_T < K = 2.6 < K_H$. (A) 0 iteration, (B) 10000 iterations, (C) 30000 iterations, (D) 100000 iterations.

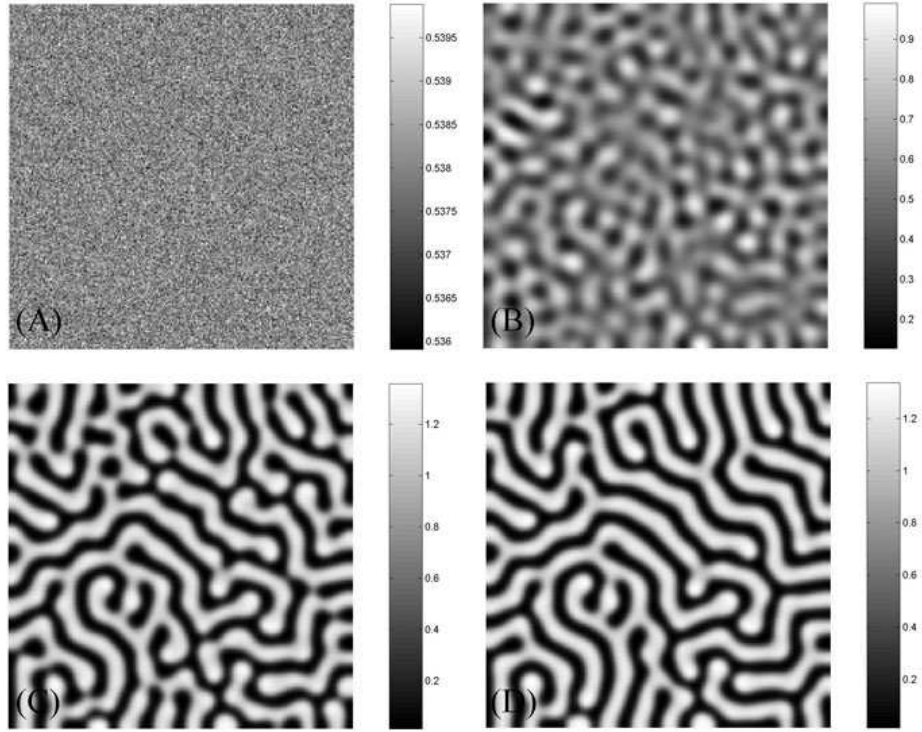


FIG. 4: Dynamics of the time evolution of the prey of model 2 with $d_1 = 0.01$, $K_T < K_H < K = 3.0$. (A) 0 iteration, (B) 20000 iterations, (C) 50000 iterations, (D) 100000 iterations.

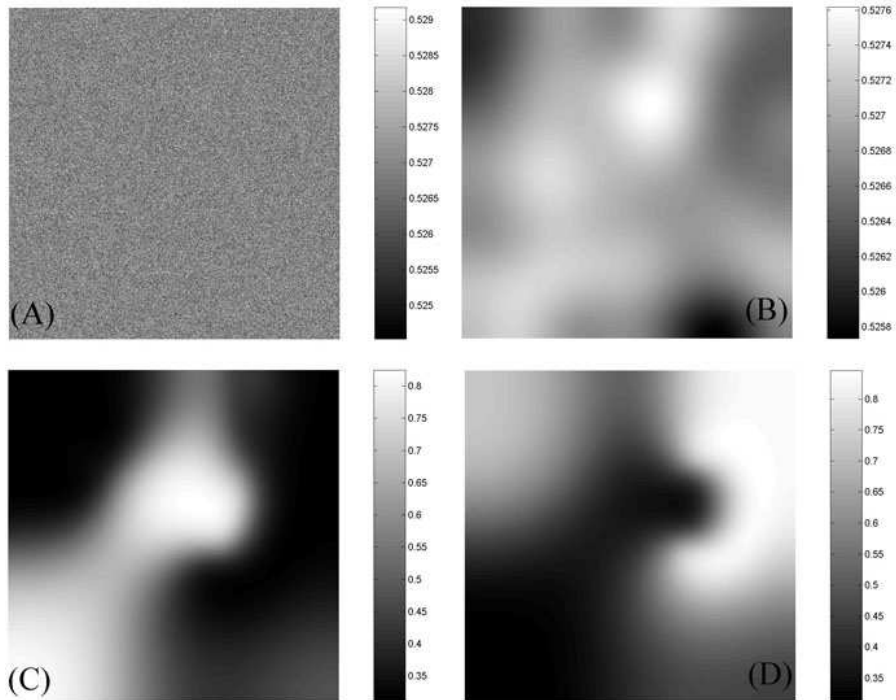


FIG. 5: Dynamics of the time evolution of the prey of model 2 with $d_1 = 0.04$, $K_T < K_H < K = 2.65$. (A) 0 iteration, (B) 30000 iterations, (C) 70000 iterations, (D) 100000 iterations.

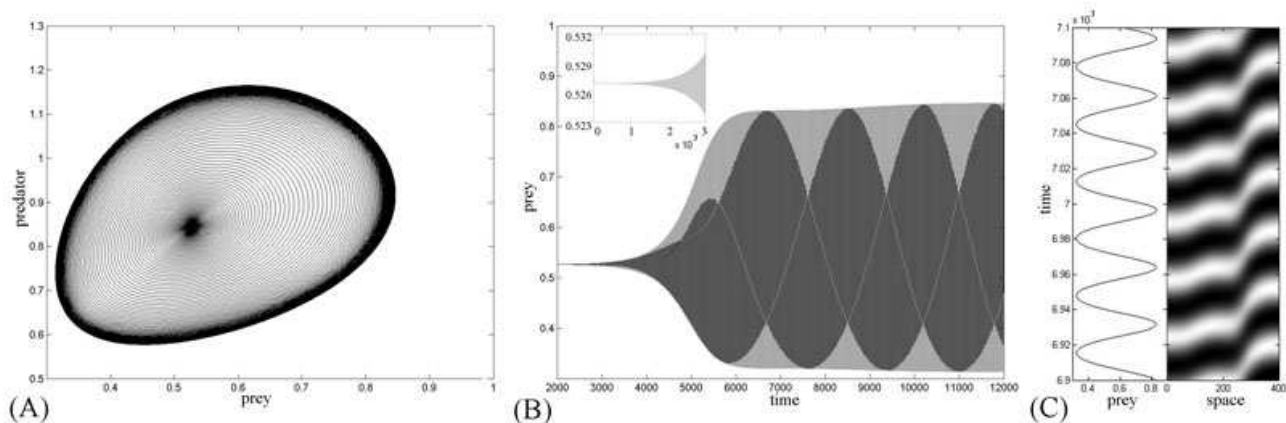


FIG. 6: Dynamical behaviors of model 2. (A) Phase portrait; (B) Time-series plot; (C) Space-time plots corresponding to Fig. 5(C). The parameters are the same as those in Fig. 5.

phase portrait (Fig. 6(A)), time series plot (Fig. 6(B)) and space-time plots (Fig. 6(C)), a one-dimensional example corresponding to Fig. 5(C). And the method of space-time plots is that let y be a constant (here, $y = 200$, the center line of each snapshots), from each pattern snapshots, choose the line $y = 200$, and pile these lines in-time-order. The space-time plots show the evolution process of the prey N throughout time t and space x . Fig. 6(A) exhibits the “local” phase plane of the system obtained in a fixed point $(0.5270, 0.8443)$ inside the region invaded by the irregular spatiotemporal oscillations, and the trajectory fills nearly the whole domain inside the limit cycle. Fig. 6(B) illustrates the evolution process of prey density with time, periodic oscillations in time finally. From Fig. 6(C), one can clearly see that a spiral wave emerges, and the system gives rise to uniform oscillations in space and periodic oscillations in time.

Comparing Fig. 2, Fig. 3 with Fig. 4, Fig. 5, we can see that the bifurcation parameter K determines the type of the pattern formation even with the same parameters, e.g., $r, \varepsilon, \beta, B, \eta, w, d_2$. In domain II of Fig. 1(A), the closer K is to K_T , the more distinct the spotted spatial pattern becomes (c.f., Fig. 2(D)). When K is much closer to K_H , the spotted and stripe-like patterns coexist (c.f., Fig. 3(D)). When K is bigger than K_H and far away from the Turing bifurcation value K_T , the distinct stripe-like pattern emerges. When K is bigger than K_H and smaller than K_T , the spiral wave pattern occurs (c.f., Fig. 5(C,D)). So we may draw a conclusion that for model 2 pure Turing instability gives birth to the spotted pattern, pure Hopf bifurcation gives birth to the spiral wave pattern, and both of them give birth to the stripe-like pattern.

4. CONCLUSIONS AND REMARKS

In this paper, we have presented a theoretical analysis of evolutionary processes that involves organisms distribution and their interaction of spatially distributed population with local diffusion. And the numerical simulations were consistent with the predictions drawn from the bifurcation analysis, i.e., Hopf bifurcation and Turing instability. In the domain II of Fig. 1(A), the stationary state of periodic spotted pattern exists when the parameters are near the Turing bifurcation line, while near the Hopf bifurcation line, both the spotted pattern and the stripe-like pattern coexist. When the parameters are located in domain III, pure Hopf instability occurs, and the spiral wave pattern emerges. When the parameters are located in domain IV, both Hopf and Turing instability occur, and the stationary state of stripe-like pattern exists.

Turing instability is relevant not only in reaction-diffusion systems, but also in describing other dissipative structures, which can be understood in terms of diffusion-driven instability. In addition to the biological relevance of Turing systems, their ability to generate structure is of great interest from the point of view of physics. There are various physical systems that show similar phenomena, although the underlying mechanisms can be very different. Thus, most of the research in the field relies on experiments and numerical simulations justified by an analytical examination. In addition, in simulations one may study pattern formation under constraints that are beyond the reach of experiments and the numerical data is also easy to analyze.

In Ref. [2], it's indicated that the basic idea of diffusion-driven instability in a reaction-diffusion model can be understood in terms of an activator-inhibitor system. And a random increase of activator species (prey, N) has a

positive effect on the creation rate of both activator and inhibitor (predator, P) species. In other words, random fluctuations may cause a nonuniform prey density. This elevated prey density has a positive effect both on prey and predator population growth rates. Following D. Alonso *et al* [2], we give the discussion to model(2). From Eqs.(2), we can obtain the following equations:

$$\frac{1}{N} \frac{\partial N}{\partial t} = r \left(1 - \frac{N}{K}\right) - \frac{\beta P}{B+N+wP}, \quad \frac{1}{P} \frac{\partial P}{\partial t} = \frac{\varepsilon \beta N}{B+N+wP} - \eta. \quad (10)$$

Similar to Ref. [2], the first equation in Eqs.(10) is a one-humped function of prey density, the numerical result can be found in [20], and prey growth rate can be increased by a higher local prey density at least in a range of parameter values. On the other hand, the second equation in Eqs.(10), i.e., predator numerical response, is an ever-increasing function of N , and high prey density always has a positive influence on predator growth. More importantly, inhibitor species (predator, P) must diffuse faster than activator species (prey, N), for an increment in inhibitor species may have a negative effect on formation rate of both species. Thus, as random fluctuations increase local prey density over its equilibrium value, prey population undergoes an accelerated growth. Simultaneously, predator population also increases, but as predators diffuse faster than prey, they disperse away from the center of prey outbreaks. If relative diffusion (d_2/d_1) is large enough, prey growth rate will reach negative values and prey population will be driven by predators to a very low level in those regions. The final result is the formation of patches of high prey density surrounded by areas of low prey density. Predators follow the same pattern.

In Ref. [11], Neuhauser and Pacala formulated the Lotka-Volterra model as a spatial one. They found the striking result that the coexistence of patterns is actually harder to get in the spatial model than in the non-spatial one. One reason can be traced to how local interaction between individual members of the species are represented in the model. In this study, our results show that the predator-prey model with Beddington-DeAngelis-type functional response and reaction-diffusion (e.g., Eqs. 2) also represents rich spatial dynamics, such as spotted pattern, stripe-like pattern, coexistence of both stripe-like and spotted pattern, spiral pattern, etc. It will be useful for studying the dynamic complexity of ecosystems or physical systems. In Ref. [9], it is indicated that reaction-diffusion models provide a way to translate local assumptions about the movement, mortality, and reproduction of individuals into global conclusions about the persistence or extinction of populations and the coexistence of interacting species. They can be derived mechanistically via rescaling from models of individual movement which are based on random walks, i.e., small random perturbation of the stationary solution (N^*, P^*) of the spatially homogeneous model (2). Reaction-diffusion system, i.e., model (2), is spatially explicit and typically incorporate quantities such as dispersal rates, local growth rates, and carrying capacities as parameters which may vary with location or time.

More interesting, when the parameters are located in domain III, pure Hopf instability occurs, and the spiral wave pattern emerges (c.f., Fig. 5, Fig. 6(C)). To our knowledge, we haven't got any report about one system that has spotted, stripe-like and spiral pattern meantime. It's well known that spirals and curves are the most fascinating clusters to emerge from the predator-prey model. A spiral will form from a wave front when the rabbit line (which is leading the front) overlaps the pursuing line of predator. The prey on the extreme end of the line stop moving as there are no predator in their immediate vicinity. However the prey and the predator in the center of the line continue moving forward. This forms a small trail of prey at one (or both) ends of the front. These prey start breeding and the trailing line of prey thickens and attracts the attention of predator at the end of the fox line that turn towards this new source of prey. Thus a spiral forms with predator on the inside and prey on the outside. If the original overlap of prey occurs at both ends of the line a double spiral will form. Spirals can also form as a prey blob collapses after predator eat into it [23, 24]. Thus, reaction-diffusion system provides a good framework for studying questions about the ways that habitat geometry and the size or variation in vital parameters influence population dynamics.

On the other hand, one can see that although there is a small difference between the denominators of the functional responses of Michaelis-Menten-type and those of Beddington-DeAngelis-type, there is an enormous gap between them in the process of computations. The Turing bifurcation expression of Michaelis-Menten-type predator-prey system is simple [64], while from (9), one can see that the Turing bifurcation analysis requires huge-sized computations, so we have to obtain more help via computers.

In fact, computer aided analysis is useful for nonlinear analysis. And computers have played an important role throughout the history of ecology. Today, numerical simulations also play an important role in spatial ecology. There are some international mathematical softwares, such as **Matlab**, **Maple**, **Mathematica**, etc. We have finished all our symbolic computations in **Maple** and obtained our pattern snapshots (i.e., numerical simulations) in **Matlab** for **Maple** is more superior in symbolic computations while **Matlab** is more superior in numerical computations.

Acknowledgments This work was supported by the National Natural Science Foundation of China (10471040) and the Youth Science Foundation of Shanxi Province (20041004).

-
- [1] Abrams, P. A., Ginzburg, L. R., 2000. The nature of predation: prey dependent, ratio dependent or neither? *Trends Ecol. Evol.* 8, 337-341.
- [2] Alonso, D., Bartumeus, F., Catalan, J., 2002. Mutual interference between predators can give rise to Turing spatial patterns, *Ecology* 83, 28-34.
- [3] Andrew M., Sergei P., Li, B.-L., 2006. Spatiotemporal complexity of patchy invasion in a predator-prey system with the Allee effect, *J.Theor. Biol.* 238, 18-35.
- [4] Arditi, R., Ginzburg, L. R., 1989. Coupling in predator-prey dynamics: Ratio-Dependence, *J. Theor. Biol.*139, 311-326.
- [5] Baumann, M., Gross, T., Feudel, U., 2007. Instabilities in spatially extended predator-prey systems: Spatio-temporal patterns in the neighborhood of Turing-Hopf bifurcations, *J. Theor. Biol.* 245, 220-229.
- [6] Beddington, J. R., 1975. Mutual interference between parasites or predators and its effect on searching efficiency, *J. Anim. Ecol.* 44, 331-340.
- [7] Berryman, A. A., 1992. The Origins and Evolution of Predator-Prey Theory, *Ecology* 73, 1530-1535.
- [8] Cantrell, R. S., Cosner, C., 2001. On the Dynamics of Predator-Prey Models with the Beddington-DeAngelis Functional Response, *J. Math. Anal. Appl.* 257, 206-222.
- [9] Cantrell, R., Cosner, C., 2003. *Spatial Ecology via Reaction-Diffusion Equations*, John Wiley & Sons, Ltd., Chichester, England.
- [10] Claudia, N., 2001. Mathematical Challenges in Spatial Ecology, *Notices of the American Mathematical Society* 47, 1304-1314.
- [11] Claudia N., Stephen W. P., 1999. An explicitly spatial version of the Lotka-Volterra model with interspecific competition, *Ann. Appl. Probab* 9, 1226-1259.
- [12] Cross, M. C., Hohenberg, P. C., 1993. Pattern formation outside of equilibrium, *Rev. Mod. Phys.* 65, 851.
- [13] Crowley P. H., and Martin, E. K., 1989. Functional responses and interference within and between year classes of a dragonfly population, *J. North Amer. Bent. Soc.* 8, 211-221.
- [14] Cui, J., Takeuchi, Y., 2006. Permanence, extinction and periodic solution of predator-prey system with Beddington-DeAngelis functional response, *J. Math. Anal. Appl.*317, 464-474.
- [15] DeAngelis, D. L., Goldstein, R. A., and Neill, R., 1975. A model for trophic interaction, *Ecology* 56, 881-892.
- [16] Dobromir T. ., Hristo V. K., 2005. Complete mathematical analysis of predator-prey models with linear prey growth and Beddington-DeAngelis functional response, *Appl. Math. Comp.* 162, 523-538.
- [17] Evelyn S., Thomas W., 2003. Pattern formation in a nonlinear model for animal coats, *J. Diff. Equa.* 191, 143-174.
- [18] Fan, M., Kuang, Y., 2004. Dynamics of a nonautonomous predator-prey system with the Beddington-DeAngelis functional response, *J. Math. Anal. Appl.* 295, 15-39.
- [19] Garvie, M. R., 2007. Finite-difference schemes for reaction-diffusion equations modelling predator-prey interactions in Matlab, *Bull. Math. Bio.* 69, 931-956.
- [20] Huisman, G., DeBoer R. J., 1997. A Formal Derivation of the “Beddington” Functional Response, *J. Theor. Biol.* 185, 389-400.
- [21] Gierer, A., Meinhardt, H., 1972. A theory of biological pattern formation, *Kybernetik* 12, 30-39.
- [22] Griffith, D. A., Peres-Neto, P. R., 2006. Spatial modeling in ecology: the flexibility of eigenfunction spatial analyses, *Ecology* 87, 2603-2613.
- [23] Gurney, W. S. C., Veitch, A. R., Cruickshank, I., McGeachin, G., 1998. Circles and spirals: population persistence in a spatially explicit predator-prey model, *Ecology* 79, 2516-2530.
- [24] Hawick, K., James, H., Scogings, C., 2006. A zoology of emergent life patterns in a predator-prey simulation model, Technical Note CSTN-015 and in Proc. IASTED International Conference on Modelling, Simulation and Optimization, September 2006, Gabarone, Botswana. 107-115.
- [25] Hassell, M. P., Varley, C. C., 1969. New inductive population model for insect parasites and its bearing on biological control, *Nature* 223, 1133-1177.
- [26] Holling, C. S., 1959. The components of predation as revealed by a study of small mammal predation of the European pine sawfly, *Cana. Ento.* 91, 293-320.
- [27] Holling, C. S., 1959. Some characteristics of simple types of predation and parasitism, *Cana. Ento.* 91, 385-395.
- [28] Hwang, T.-W., 2003. Global analysis of the predator-prey system with Beddington-DeAngelis functional response, *J. Math. Anal. Appl.* 281, 395-401.
- [29] Jost, C., 1998. Comparing predator-prey models qualitatively and quantitatively with ecological time-series data, PhD-Thesis, Institute National Agronomique, Paris-Grignon.
- [30] Jost, C., Arino, O., Arditi, R., 1999. About deterministic extinction in ratio-dependent predator-prey models, *Bull. Math. Biol.*61, 19-32.
- [31] Just, W., Bose, M., Bose, S., Engel, H., Schöll, E., 2001. Spatiotemporal dynamics near a supercritical Turing-Hopf bifurcation in a two-dimensional reaction-diffusion system, *Phys. Rev. E* 64, 026219.
- [32] Kar, T. K., and Pahari, U. K., 2007. Modelling and analysis of a prey-predator system with stage-structure and harvesting, *Nonl. Anal.: Real World Appl.* 8, 601-609.
- [33] Karen P., Maini, P. K., Nicholas, A.M., 2003. Pattern formation in spatially heterogeneous Turing reaction-diffusion models, *Phys. D* 181, 80-101.
- [34] Klausmeier, C. A., 1999. Regular and Irregular Patterns in Semiarid Vegetation, *Science* 284, 1826-1828.

- [35] Kuang, Y., Beretta, E., 1998. Global qualitative analysis of a ratio-dependent predator-prey system, *J. Math. Biol.* 36, 389–406.
- [36] Lejeune, O., Tlidi, M., Couteron, P., 2002. Localized vegetation patches: A self-organized response to resource scarcity, *Phys. Rev. E* 66, 010901.
- [37] Leppänen, T., 2004. Computational studies of pattern formation in Turing systems, Phd-thesis, Helsinki University of Technology, Finland.
- [38] Leppänen, T., Karttunen, M., Barrio, R. A., Kaski, K., 2004. Morphological transitions and bistability in Turing systems, *Phys. Rev. E* 70, 066202.
- [39] Levin, S. A., 1992. The Problem of Pattern and Scale in Ecology, *Ecology* 73, 1943-1967.
- [40] Levin, S. A., Grenfell, B., Hastings, A., Perelson, A. S., 1997. Mathematical and Computational Challenges in Population Biology and Ecosystems Science, *Science* 275, 334-343.
- [41] Levin, S. A., Segel, L. A., 1976. Hypothesis for origin of planktonic patchiness, *Nature* 259, 659.
- [42] Li, Z., Wang, W., Wang, H., 2006. The dynamics of a Beddington-type system with impulsive control strategy, *Chaos, Solitons and Fractals* 29, 1229-1239.
- [43] Liu, Q., Jin, Z., Liu, M., 2006. Spatial organization and evolution period of the epidemic model using cellular automata, *Phys. Rev. E* 74, 031110.
- [44] Liu, Q., Jin, Z., 2007. Formation of spatial patterns in epidemic model with constant removal rate of the infectives, *J. Stat. Mech.* P05002.
- [45] Liu, R. T., Liaw, S. S., and Maini, P. K., 2006. Two-stage Turing model for generating pigment patterns on the leopard and the jaguar, *Phys. Rev. E* 74, 011914.
- [46] Liu, S., Edoardo B., 2006. A stage-structured predator-prey model of Beddington-Deangelis type, *SIAM J. Appl. Math.* 66, 1101-1129.
- [47] Maini, P. K., 2004. Using mathematical models to help understand biological pattern formation, *Comp. Rend. Biol.* 327, 225-234.
- [48] Maini, P. K., Baker, R. E., and Chuong, C., 2006. The Turing model comes of molecular age, *Science* 314, 1397-1398.
- [49] Maionchi, D. O., Reis, S. F., Aguiar, M. A. M., 2006. Chaos and pattern formation in a spatial tritrophic food chain, *Ecol. Model.* 191, 291-303.
- [50] Medvinsky, A., Petrovskii, S., Tikhonova, I., Malchow, H., Li, B-L., 2002. Spatiotemporal complexity of plankton and fish dynamics, *SIAM Review* 44, 311-370.
- [51] Murray, J., 2003. *Mathematical Biology II: Spatial Models and Biomedical Applications*. Springer, Berlin.
- [52] Ouyang, Q. Swinney, H. L., 1991. Transition from a uniform state to hexagonal and striped Turing patterns, *Nature* 352, 610-612.
- [53] Pascual, M., 1993. Diffusion-induced chaos in a spatial predator-prey system, *Proc. Roy. Soc. Lond. B* 251, 1-7.
- [54] Pascual, M., Roy, M., Franc, A., 2002. Simple temporal models for ecological systems with complex spatial patterns, *Ecol. Lett.* 5, 412-419.
- [55] Ruan, S., Xiao, D., 2001. Global Analysis in a Predator-Prey System with Nonmonotonic Functional Response, *SIAM J. Appl. Math.* 61, 1445-1472.
- [56] Segel, L. A., Jackson, J. L., 1972. Dissipative structure: An explanation and an ecological example, *J. Theor. Biol.* 37, 545-559.
- [57] Seydel, R., 1994. *Practical bifurcation and stability analysis*, Springer, New York.
- [58] Shuji I., Kunihiko K., 2006. Turing pattern with proportion preservation, *J. Theo. Ecol.* 238, 683-693.
- [59] Skalski, G. T., Gilliam, J. F., 2001. Functional responses with predator interference: Viable alternatives to the Holling type II model, *Ecology* 82, 3083-3092.
- [60] Arecchi, F. T., Stefano Boccaletti, and PierLuigi Ramazza, 1999. Pattern formation and competition in nonlinear optics, *Phys. Repo.* 318, 1-83.
- [61] Turing, A. M., 1952. The chemical basis of morphogenesis, *Phil. Trans. R. Soc. London B* 237, 7-72.
- [62] Vanag, V. K., Yang, L., Dolnik, M., Zhabotinsky, A. M., Epstein, I. R., 2000. Oscillatory cluster patterns in a homogeneous chemical system with global feedback, *Nature* 406, 389-391.
- [63] Von Hardenberg, J., Meron, E., Shachak, M., Zarmi, Y., 2001. Diversity of Vegetation Patterns and Desertification, *Phys. Rev. Lett.* 87, 198101.
- [64] Wang, W., Liu, Q., and Jin, Z., 2007. Spatiotemporal complexity of a ratio-dependent predator-prey system, *Phys. Rev. E* 75, 051913.
- [65] Wang, W., Wang, H., Li, Z., 2007. The dynamic complexity of a three-species Beddington-type food chain with impulsive control strategy, *Chaos, Solitons and Fractals* 32, 1772-1785.
- [66] Yang, L., Dolnik, M., Zhabotinsky, A. M., Epstein, I. R., 2002. Pattern formation arising from interactions between Turing and wave instabilities, *J. Chem. Phys.* 117, 7259-7265.
- [67] Yang, L., Dolnik, M., Zhabotinsky, A. M., Epstein, I. R., 2002. Spatial Resonances and Superposition Patterns in a Reaction-Diffusion Model with Interacting Turing Modes, *Phys. Rev. Lett.* 88, 208303.
- [68] Yang, L., Irving R. E., 2003. Oscillatory Turing Patterns in Reaction-Diffusion Systems with Two Coupled Layers, *Phys. Rev. Lett.* 90, 178303.
- [69] Yang, L., Irving R. E., 2004. Symmetric, asymmetric, and antiphase Turing patterns in a model system with two identical coupled layers, *Phys. Rev. E* 69, 026211.
- [70] Yang, L., Milos D., Anatol M. Z., Irving R. E., 2006. Turing patterns beyond hexagons and stripes, *Chaos* 16, 037114.

